1969-06

Experimental techniques for analysis of transverse impact on beams

Berns, Thomas Herbert

Monterey, California. U.S. Naval Postgraduate School

EXPERIMENTAL TECHNIQUES FOR ANALYSIS OF TRANSVERSE IMPACT ON BEAMS

by

Thomas Herbert Berns

United States
Naval Postgraduate School

THESIS

EXPERIMENTAL TECHNIQUES FOR ANALYSIS OF

TRANSVERSE IMPACT ON BEAMS

by

Thomas Herbert Berns

June 1969

Experimental Techniques for Analysis of Transverse Impact on Beams

by

Thomas Herbert Berns
Lieutenant (junior grade), United States Navy
B.S., United States Naval Academy, 1968

Submitted in partial fulfillment of the
requirements for the degree of

MASTER OF SCIENCE IN MECHANICAL ENGINEERING

from the

NAVAL POSTGRADUATE SCHOOL
June 1969

ABSTRACT

Procedures are developed to facilitate laboratory investigation of the effects of short-duration transverse impact loading on simply supported beams. The particular beam investigated was aluminum, with constant rectangular cross-section. Six loading conditions were examined, consisting of a central impact from three heights for each of two spherical masses. Theoretical analysis was made of the frequency and deflection characteristics for ten equally spaced locations on the beam, under the assumption of Euler's beam theory. Experimental data were compared with theoretical values to give an indication of the effectiveness of the theoretical system in representing the physical system. It was concluded that the theory gives a good representation of the physical system, especially with respect to the frequency characteristics.

The experimental work was performed from January, 1969 through May 1969, at the Naval Postgraduate School, Monterey, California.

TABLE OF CONTENTS

LIST OF TABLES

LIST OF ILLUSTRATIONS

SYMBOLS

English Letter Symbols

a	Beam frequency constant, $a^4 = EI/\rho A$
A	Beam cross-sectional area
b	Beam depth
E	Young's modulus of elasticity
f	Frequency of vibration
F	Gage factor
g	Gravitational constant
G_i	$a^2 \zeta_i^2 E_i A_i \cos \frac{1}{2} \zeta_i L$
h	Beam thickness
I	Moment of inertia
L	Beam length
m_1	Beam mass
m_2	Striker mass
m_t	Test specimen mass
$\overline{m}$	Combined mass of beam and striker
M	Ratio m_1/m_2
M_B	Bending moment
P	Concentrated force
R	Resistance, electrical
s	Striker drop height
t	Time
T	Function dependent on t, used in the assumed expression for y(x,t)
v_{20}	Striker velocity at impact

V	Shear force
$\mathcal{V}$	Volume
w	Distributed load per unit length
W	Weight
x	Horizontal distance from support
X	Function dependent on x
y	Vertical displacement, positive downward

Greek Letter Symbols

ϵ	Normal strain
ν	Poisson's ratio
ς	Arbitrary constant
ρ	Mass density
σ	Normal stress
τ	Period of vibration; decay constant
ϕ	$\frac{1}{2}\varsigma L$
ω	Natural (angular) frequency of vibration
Ω	Ohm

Subscripts

b	Beam
B	Bending
i	Index
max	Maximum
t	Test specimen
x	Coordinate along beam
z	Horizontal coordinate perpendicular to x

1	Beam
2	Striker
20	Striker at impact

ACKNOWLEDGEMENT

The author extends his gratitude to Professor E. F. Lynch of the Department of Mechanical Engineering, Naval Postgraduate School, for his advice and encouragement throughout the investigation. Indebtedness is also due Mr. Ray Garcia, of the Mechanical Engineering Department machine shop, whose knowledge of electronics was invaluable in the instrumentation of the working model.

I. INTRODUCTION

The word impact denotes the collision of two or more bodies. The phenomenon is shock-like because it occurs in a very short time interval. During this time the colliding bodies experience an application of intense force and there is a considerable exchange of energy. When one of the bodies is rounded or pointed, the area of collision is extremely small. Because the disturbances are propagated away from the point of impact, different locations are not subjected to the same forces at the same time.

When a beam is struck by a sphere, the beam will vibrate at frequencies dependent upon the properties of the beam and independent of the properties of the sphere. The displacement and stresses in the beam, however, are dependent upon the properties of both the beam and the sphere. Thus impact loading, as opposed to impulsive loading, must take into consideration not only the properties of the beam, but also the mass, velocity, location of application, and mass ratio with respect to the beam, of the striking body.

The problem of spherical impact loading at the center of a uniform simply supported beam has been treated analytically by Goldsmith [5]*, whereby a suitable boundary condition is substituted into the equation of free vibration of the beam in order to account for the applied impact.

Little published data for this type of problem are available. What was found gave only a scant description of equipment and almost no information about procedure and sources of error. The major portion of the effort expended on this project was toward the design and construction of suitable testing equipment.

---

*Numbers in brackets refer to publications listed on page 63.

II. OBJECTIVES

This project was undertaken with the following objectives:

a. Examine the validity of previously developed analytical expressions for the reaction of the beam at various locations and various times after impact.

b. Develop laboratory procedures for experimentally carrying out objective (a).

c. Examine various methods of obtaining data from the working model, and determine the feasibility of each.

d. Design and construct a test rig that can easily be used for the investigation of beams with parameters differing from those of the beam studied.

III. DESCRIPTION OF TEST EQUIPMENT

A. MECHANICAL COMPONENTS

The beam investigated was designed to be simply supported. The actual testing rig was made to approach the ideal, theoretical "point loading" at either end. To avoid having the beam fall from its supports whenever struck, it was necessary to have an overhang beyond the supports. An overhang of ¼ inch at each end assured that the beam would remain on the supports. The amount of overhang was less than one per cent of the distance between the supports. To ensure that the beam, once struck by the sphere, did not bounce at its ends, it was necessary to support it with knife edges on both the upper and lower surfaces. To minimize axial strains in the beam, one end was provided with rollers to permit a changing horizontal distance between the supports. The aluminum beam was sufficiently soft that knife edges of the supports could be constructed of ordinary steel. No special hardening process was needed after fabrication to retain their sharpness.

The roller mechanism was constructed as follows: The knife edges at the moving end of the beam were attached to steel plates, providing a flat, horizontal surface for ball bearings. Two additional flat plates provided the second contact surfaces for the ball bearings. These outermost plates had shallow grooves parallel to the beam, in order to preserve the longitudinal alignment of the ball bearings. Both upper and lower sets of bearings consisted of four ½ inch steel balls whose relative positions were maintained by a small piece of sheet metal with punched holes appropriately spaced.

The entire test rig (beam, knife edges, and roller mechanism) was bolted to a massive wide-flange support beam. This beam, bolted down, provided a solid foundation and ensured that the two ends of the test beam were properly aligned.

Several methods were investigated to determine the best method of propelling the sphere onto the midpoint of the beam. An attempt was made to mount the beam vertically and strike it with the sphere moving horizontally. This was accomplished by using the sphere as a pendulous mass. Knowledge of the release height and the length of the string permitted calculation of the velocity at impact. This method of collision had the advantage of simple retrieval of the sphere after impact. Unfortunately, although the effects of gravity were not part of the theoretical analysis of the problem, it was found that the weight of the roller mechanism made vertical mounting prohibitive. With horizontal mounting of the beam thus made necessary, the problem became one of vertical loading, the primary difficulty of which was retrieving the sphere. One possible drop method was to suspend the sphere over the contact point by means of an electromagnet. The current could be stopped instantly and the sphere would then fall freely. Difficulties arose, however, in trying to get enough magnetic force to hold the sphere. Because of its geometry, the sphere had only a minute area for contact with a flat magnetic surface. The only ways to increase this area were to hollow out an indentation in the electromagnet of radius equal to that of the sphere, or to use a tube-like electromagnet of radius less than that of the sphere to give a circle of contact. None of the foregoing methods proved very feasible, due to economic reasons. The dropping procedure finally decided upon was: A ½ inch aluminum plate was mounted above the test beam. In this plate was

drilled a 3/4 inch diameter hole which was positioned by means of a plumb bob in such a manner that a point on its periphery was directly over the contact point. This location on the circumference of the hole was marked. A length of string was attached to a small eye welded to the sphere. By leading the string through the hole and then along the top of the plate away from the centerline of the hole, the sphere could be raised to any desired height above the point of contact with the test beam. With the string clamped to the plate, release was accomplished by cutting the string. The string was cut by laying a blade of a scissors under the horizontal portion of the string atop the aluminum plate. When this procedure was followed, the sphere was suddenly released upon cutting and was not jarred. The mass of the length of string was, of course, negligible, compared to that of the sphere. Another short piece of string was tied to the eye of the sphere so that the retrieval of the sphere was accomplished by yanking this slack string after the sphere impacted the beam only once. It should be mentioned that since the sphere did not rotate before impingement on the beam, the eye did not interfere with the collision.

B. ELECTRICAL COMPONENTS

In order to measure the strain during bending, electrical resistance strain gages were employed. The gages were SR4, type A5, having a resistance of 120.4$\Omega \pm 1\%$. Although type C gages would have increased the response, the main reason for choosing the gages that were used was that they were available in quantity. Strain gage rosettes were found to be unnecessary for the problem under consideration, since the principal axis of strain was known to be along the length of the beam. The gage locations on the beam are given in Table I. Gages were placed at ten different distances from the midpoint of the beam. One gage was at the midpoint,

a second 2½ inches away, and the remainder were spaced every five inches from the first two, going toward the two ends of the beam. Having a gage every five inches from the center on one half of the beam and every five plus 2½ inches on the other half of the beam achieved the effect, assuming that each half of the beam responded similarly, of having a gage every 2½ inches on one half of the beam only. Since the foregoing assumption is an important one, a means of checking the comparative response of the two halves of the beam was provided. An eleventh, testing gage was placed on the beam at a distance from the center equal to that of one of the ten gages studied. This testing gage and its equidistant counterpart were then compared from time to time in order to verify the assumption of symmetry of response.

Bridges were built consisting of two active and two compensating gages. The active gages were placed above and below the test point in order to give double amplification of the resistance changes. The compensating gages were affixed to a slab of aluminum identical to the test beam material. The wiring of the bridges was such that the bulk of the connectors was on the slab having the compensating gages, thus minimizing the amount of wire that was on the test beam. The bridge wiring is shown in Fig. 4.

The bridges were connected to a Honeywell Model 130-2C Carrier Amplifier, which relayed the strain signals to a Honeywell Model 906C Visicorder Oscillograph. The Visicorder Oscillograph uses galvanometers to interpret the signals received from the amplifier and has as its output the deflection of a beam of ultraviolet light, whose motion is recorded on light-sensitive paper. Fig. 5 shows the overall wiring diagram of the experimental setup, from strain gages to final output.

IV. EXPERIMENTAL PROCEDURE

The test beam was examined under six different loading conditions. Two striker masses were used, with values of 97.0g and 493.5g. Drop heights of six, three, and one and a half inches, corresponding to striking velocities of 5.68, 4.02, and 2.84 feet per second, respectively, were used.

The striker masses were determined using the Ohaus balance. The accuracy of the balance was verified with known masses of various magnitudes.

Obtaining the proper drop height was done as follows: A block was placed beneath the test beam in its unloaded state to prohibit downward deflection. A second block of height equal to the desired drop height was placed over the point of impact. The sphere was then lowered until it just touched the second block, and the string suspending the sphere was then clamped to the suspension plate.

The Visicorder Oscillograph was set at a paper speed of ten inches per second and the time line selector was set to give time spacings of .01 second. The Carrier Amplifier was balanced according to the technical manual before every drop, and also afterwards, to check if the gage voltage had wavered. The A-CALIBRATE switch on the amplifier was set at the "0" position. Because the light trace deflections on the Visicorder Oscillograph were rather small, the amplifier was set at full gain. The output of the amplifier remained in the linear region at the full gain position. Because the acceleration of the recording paper from zero to ten inches per second took place in a finite time interval, this machine was started before the sphere was released. The various light traces, which appeared as small dots when the test beam was not loaded, were set

on the heavier of the reference gridlines. These sharp, narrow lines were .1 inch apart, with the heavier of the gridlines at .5 inch intervals along the six inch width of the record.

Calibration of the galvanometer spots was made by imposing a static load on the test beam. A simple calculation gave the value of the strain for the known load. The dynamic records were thereafter compared to the deflection results obtained from static loading.

The modulus of elasticity and Poisson's ratio for the test beam were determined using a specimen from the same stock as test beam. This specimen was subjected to pure bending. Knowledge of the incremental strains and the incremental loading which caused them, coupled with the geometry of the specimen, led to a calculation of the two aforementioned properties. For this test, gages identical to those on the test beam were used. The recording instrument used was an Ellis Associates Bridge Amplifier Meter, model BAM-1. Strains were measured during both loading and unloading, the results indicating no residual stresses.

At a given end of the test beam, the knife edges had to be flush with the beam, but care was taken to tighten them no more than necessary to meet this condition. Further tightening resulted in clamping, rather than simply supporting, the end of the test beam. After each drop, the bolts connecting opposing knife edges were checked for any loosening. If this occurred, the run was repeated. To make sure that the force transmitted through the knife edges to the line of contact with the end of the test beam was uniformly distributed, the beam and the knife edge plates were repeatedly checked with a level in two perpendicular directions.

A final check that was made to compare the "before and after" conditions concerned the galvanometer light traces. Occasionally, with the

larger sphere and the greatest drop height, the shock upon impact caused the zero strain position of the light to jump about .1 inch and remain there. If such was the case, the run was repeated. The observation just described was due to the Visicorder Oscillograph itself and was not an indication of any residual stresses in the test beam.

V. THEORETICAL CONSIDERATIONS

Consider a vibrating beam of uniform cross-section. The governing equation for the vibration of an incremental section dm_1 of the beam is given by the well-known relationship

$$\frac{\partial^4 y}{\partial x^4} = -\frac{w}{g}\frac{1}{EI}\frac{\partial^2 y}{\partial t^2} \quad , \tag{1}$$

where the term w/g is equal to the mass of the section under consideration. The expression for y, the positive downward deflection, as a function of x and t may be taken as

$$y(x,t) = X_i(x)\,T_i(t) \quad . \tag{2}$$

This expression, substituted into Eq. (1), yields:

$$X_i''''(x)\,T_i(t) = -\frac{w}{g}\frac{1}{EI}\,X_i(x)\,\ddot{T}_i(t) \quad . \tag{3}$$

Now, the term w/g may be replaced by its equivalent ρA. Making this substitution and separating the variables $X_i(x)$ and $T_i(t)$,

$$\frac{X_i''''}{X_i} = -\frac{\rho A}{EI}\frac{\ddot{T}_i}{T_i} \quad . \tag{4}$$

Further, define $a = \sqrt[4]{EI/\rho A}$ so that

$$\frac{X_i''''}{X_i} = -\frac{1}{a^4}\frac{\ddot{T}_i}{T_i} = \zeta_i^4 = \text{constant} \tag{5}$$

where $\zeta_i^2 a^2 = \omega_i$ has the dimensions of frequency.

The general solution of Eq. (5) is

$$y(x,t) = \sum_{i=1}^{\infty}(A_i \sin \zeta_i x + B_i \cos \zeta_i x + C_i \sinh \zeta_i x + D_i \cosh \zeta_i x)(E_i \sin \omega_i t + F_i \cos \omega_i t) \quad , \tag{6}$$

where the summation extends over all i for which ζ_i is a solution of Eq. (5), determined with appropriate boundary conditions.

To apply Eq. (6) to the case when the center of the beam is struck by a sphere, the applicable boundary condition, according to Goldsmith [5], is that the discontinuity in shear at the center of the beam is equal to the reversed effective force of the striker. From the diagram below, the relationship is

$$EI \frac{d^3y}{dx^3} = \frac{1}{2} m_2 \frac{d^2y}{dt^2} , \qquad \text{at } x = L/2,\ t = t. \quad (7)$$

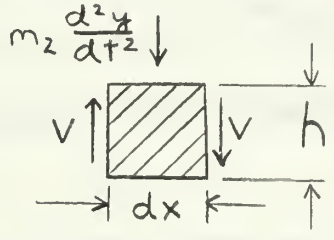

Using the conditions of symmetry on either side of the central point of impact, the remaining boundary conditions are:

$$y = 0 , \qquad \text{at } x = 0,\ t = t \quad (8)$$

$$\frac{d^2y}{dx^2} = 0 , \qquad \text{at } x = 0,\ t = t \quad (9)$$

$$\frac{dy}{dx} = 0 , \qquad \text{at } x = L/2,\ t = t. \quad (10)$$

The boundary conditions (8-10) give

$$F_i = B_i = D_i = 0$$

and

$$C_i = - A_i \frac{\cos \frac{1}{2} \zeta_i L}{\cosh \frac{1}{2} \zeta_i L} . \quad (11)$$

Equation (6) now becomes

$$y(x,t) = \sum_{i=1}^{\infty} \frac{1}{a^2 \zeta_i^2} G_i X_i \sin \zeta_i^2 a^2 t , \quad (12)$$

valid for both halves of the beam for $0 \leq x \leq \frac{L}{2}$, where

$$G_i = a^2 \zeta_i^2 E_i A_i \cos \frac{1}{2} \zeta_i L \quad (13)$$

and $$X_i = \left[\frac{\sin \zeta_i x}{\cos \frac{1}{2} \zeta_i L} - \frac{\sinh \zeta_i x}{\cosh \frac{1}{2} \zeta_i L} \right] . \qquad (14)$$

Substituting Eq. (12) into Eq. (7) yields:

$$\tfrac{1}{2} \zeta_i L \left(\tan \tfrac{1}{2} \zeta_i L - \tanh \tfrac{1}{2} \zeta_i L \right) = 2 \frac{m_1}{m_2} .$$

Or, defining $\varphi_i = \frac{1}{2} \zeta_i L$ and $M = \frac{m_1}{m_2}$,

$$\varphi_i \left(\tan \varphi_i - \tanh \varphi_i \right) = 2M . \qquad (15)$$

The roots of Eq. (15) are given in Table 2 for i from one through seven.

The evaluation of G_i requires that the impact force be replaced by an initial velocity condition. If, as assumed by Goldsmith [5], the striking mass m_2 imparts, at the instant of contact, a velocity to the elemental beam section, dm_1, that is approximately equal to v_{20}, then, by conservation of momentum,

$$m_2 v_{20} \approx (m_2 + dm_1) v_{20} \; ; \; \int \left. \frac{dy}{dt} \right|_{(x,0)} d\bar{m} = m_2 v_{20} , \qquad (16)$$

where the integration $d\bar{m}$ is with respect to the total mass of the beam and striker.

From Eq. (12), $\left. \frac{dy}{dt} \right|_{x=0} = \sum_{i=1}^{\infty} G_i X_i$, defined as $\psi(x)$. Multiplying by X_j, there results (17)

$$\sum_{i=1}^{\infty} G_i X_i X_j = \psi(x) X_j . \qquad (18)$$

If Eq. (18), multiplied by m_2 and evaluated at x = L/2 is added to the integral of the same equation with respect to the beam mass $dm_1 = m_1 dx/L$, there results $\sum_{i=1}^{\infty} G_i \left\{ \frac{2m_1}{L} \int_0^{L/2} X_i X_j \, dx + m_2 X_i X_j \right\}$

$$= \left\{ \frac{2m_1}{L} \int_0^{L/2} X_j \psi(x) \, dx + m_2 X_j \psi\left(\tfrac{L}{2}\right) \right\} , \qquad (19)$$

where the variables in the terms involving m_2 are evaluated at $x = L/2$.

Equation (19), as in the case of Eq. (16), represents an integration with the total mass. For $i \neq j$, the left hand side of Eq. (19) equals zero, by direct integration. Hence, for $i = j$,

$$G_i = \frac{\frac{2m_1}{L}\int_0^{L/2} X_i \psi(x)\,dx + m_2 X_i \psi(\frac{L}{2})}{\frac{2m_1}{L}\int_0^{L/2} X_i^2\,dx + m_2 X_i^2}\ , \qquad (20)$$

where, again, the variables in the terms involving m_2 are evaluated at $x = L/2$. Going back to the assumption made after Eq. (15), the following conditions for the instant of impact may be written:

$$\frac{dy}{dt} = 0 \quad \text{at } x \neq L/2,\ t = 0 \qquad (21)$$

$$\frac{dy}{dt} = v_{20} \quad \text{at } x = L/2,\ t = 0\ . \qquad (22)$$

Using these initial conditions,

$$G_i = \frac{m_2 v_{20} X_i|_{x=L/2}}{\frac{2m_1}{L}\int_0^{L/2} X_i^2\,dx + m_2 X_i|_{x=L/2}}$$

$$= \frac{4v_{20}}{\varphi_i\left(\frac{1}{\cos^2\varphi_i} - \frac{1}{\cosh^2\varphi_i}\right) + \frac{2M}{\varphi_i}}\ . \qquad (23)$$

Substituting in Eq. (12) for G_1 yields the equation for the deflection of the beam:

$$y(x,t) = \frac{L^2 v_{20}}{a^2}\sum_{i=1}^{\infty}\frac{1}{\varphi_i^3}\left\{\frac{\frac{\sin 2\varphi_i x/L}{\cos\varphi_i} - \frac{\sinh 2\varphi_i x/L}{\cosh\varphi_i}}{\frac{1}{\cos^2\varphi_i} - \frac{1}{\cosh^2\varphi_i} + \frac{2M}{\varphi_i^2}}\right\}\sin\frac{4\varphi_i^2 a^2}{L^2}t \qquad (24)$$

The above expression is valid for $0 \leq x \leq \frac{L}{2}$ and this is all that is required since the response is symmetrical with respect to $x = L/2$.

Since the system under investigation will not vibrate for an indefinite period of time, the amplitude of vibration for a given location is subject to internal and external damping forces. The net effect of these damping forces can be approximated by an exponential decay. The ratio of the amplitude at any time to the initial amplitude is given by $e^{-t/\tau}$, where τ is the time constant of decay. The time t required for the amplitude to reach 36.8% of its initial value is the time constant of decay. The method of determining τ from the Visicorder Oscillograph record is shown in Fig. 15.

VI. SUMMARY OF EXPERIMENTAL RESULTS

It was noted that the theoretical development of the problem gave the deflection y as a function of x and t. The experimental procedure, however, measured strain as a function of x and t. In order to correlate the two, proportionality of bending strain to the curvature at any chosen location and time was used.

Figures 7 through 12 depict the maximum deflection at each gage location for each of the six loading conditions investigated. In each of these figures, as the parameter x/L increased, there was a fairly constant increase in the maximum strain until the value of x/L was approximately .17. Between this value and .3, there was very little increase in the maximum strain. Proceeding toward the midpoint of the beam, the strain once again increased, but at a higher rate. This higher rate of strain increase as the midpoint of the beam was neared can be explained by examination of Eq. (24). The strain is proportional to the second derivative of y with respect to x. When this derivative is taken, both the sin and sinh terms of the numerator are negative. The sinh term, with its rapid increase as the argument is increased, is the major contributing term to the deflection y. Hence, the high rate of increase in strain as L/2 is approached is explained. The region of approximately constant strain is explained by Fertis and Zobel [4]: The second harmonic has a node at x/L = .25. This fact, coupled with the fact that the lower order harmonics contribute to the deflection more than the higher order harmonics, explains the decrease in the slope of the deflection-x/L curve near x/L = .25. Comparison of Figs. 7-9 for the smaller sphere with Figs. 10-12 for the larger sphere shows

that the runs made with the larger sphere, whose momenta were greater than the momenta of the smaller sphere, resulted in a much higher maximum strain near the center of the beam, while at the same time, the maximum strains near the end of the beam were only about twice as great for a particular drop height. This observation is explained once again in the sinh term of Eq. (24), where the ϕ_i in the argument are larger for the larger sphere.

Figure 13 shows the deflection at the center of the test beam for the two striking masses used, plotted as a function of the striking velocity. The linear relationship of the two quantities was shown to hold quite well in the experimental analysis of the problem.

The available literature indicated that the higher order frequencies of vibration are expected to attenuate rapidly. Figures 14 and 15 were plotted in order to determine what parameters affect the length of time that these frequencies are discernable. It was observed that the duration increased with the velocity of the striker and decreased with the mass of the striker.

It was possible to determine the first three natural modes of vibration by visual inspection of the Visicorder Oscillograph tapes. The manner in which this was done is shown in Fig. 16. For the smaller striker, the first three frequencies were found to be: 9.1, 33.3, and 83.4 cycles per second. For purposes of comparison, the theoretical values were, respectively, 8.47, 33.9, and 76.4 cycles per second. For the larger striker, the experimental values were 11.75, 50.0, and 100.0 cycles per second, and the respective theoretical values 11.9, 47.6, and 107.0 cycles per second. The difference in frequencies for the two strikers is due to the fact that, since the striker is a part of the

vibrating system for a finite time interval, there is a different system for each striker.

The time constant of decay was determined for the fundamental frequency and was essentially the same for both striking masses. The value of τ was found to be $\tau = 2.65$ seconds.

VII. CONCLUSIONS

The conclusions to be drawn from this investigation are summarized as follows:

1. The experimental test rig was a good approach to the ideal simply supported beam. This was partially evidenced by the fact that there was no noticeable damping of vibration due to the roller mechanism; also, the angular deflection at the ends of the test beam was sufficiently small that the clamped end effect was negligible.

2. The shape of the experimental curves of Figs. 7 through 12 is very close to that predicted by theory, but, for most of the positions studied, the experimental curves were low by up to 15 per cent. This indicates that there is a constant source of error that affects only the magnitude of the deflection. Although the cause of this error could not be determined, an awareness of it can be applied to future experimental data.

3. For the test beam used, the ratio of maximum deflection to the length of the beam was so small that only the half sine wave mode of deflection could be observed visually, and the value of a more detailed analysis with stroboscopic lighting did not justify the additional effort necessary.

4. The strain-indicating components discussed earlier appear to be quite satisfactory.

5. Some of the improvements suggested in the following section should increase the degree of agreement with the theoretical results, since even without these improvements the experimental-theoretical correlation was good.

6. The repeatability of test conditions indicated that the loading shock did not affect the support conditions at the ends of the test beam during a particular run.

7. It is concluded that the test rig developed in this investigation is suitable for use in the investigation of beams of variable cross-section, as long as the end dimensions of such beams are close to the end dimensions of the beam used in this investigation.

VIII. RECOMMENDATIONS FOR ADDITIONAL INVESTIGATIONS

1. With the test rig as designed, many variations can be made in the loading of the test beam. Some possibilities are:

    a. Use drop masses of a compressible nature, such as rubber balls.

    b. Load the test beam at locations other than at the center.

    c. Use a drop mass which sticks to the beam after collision.

    d. Examine the response to forced vibration, of a sinusoidal or a hammering nature.

    e. Examine the response of the test beam to a plucking action.

2. Build a test beam of a different material.

3. Build a test beam of a non-uniform cross-sectional area.

4. Replace the single lower gage at A with two gages to conform to the bridges at the other stations.

5. Increase the amplitude of the strain signal, possibly by using different types of strain gages.

6. Use wire of smaller rigidity for the connections from the active to the compensating gages, as stiffer wire tends to dampen the motion of the test beam.

7. Make a spectral analysis of the waveform of the output in order to examine the first "x" number of terms in the infinite series of the theoretical analysis of the problem.

8. Determine the energy added to the beam by the striker by measuring the striker rebound height, and apply this information to an explanation of conclusion number two, page 30.

TABLE I

Strain Gage Locations

Station	(L/2 - x), inches	x/L
A	0.0	.5000
B	2.5	.4519
C	5.0	.4038
D	7.5	.3557
E	10.0	.3076
F	12.5	.2595
G	15.0	.2114
H	17.5	.1633
I	20.0	.1152
J	22.5	.0671
Z (check)	10.0	.3076

TABLE II

Values of φ_i , i=1.7 in Equation (15)

	M=8.80	M=1.73
φ_1	1.319	1.57
φ_2	4.237	4.71
φ_3	7.280	7.85
φ_4	10.370	10.99
φ_5	13.480	14.13
φ_6	16.600	17.27
φ_7	19.726	20.41

TABLE III

Definition of Terms Used in Computer

Solution of Equation (24)

FI	φ_i
FIXL	$2\varphi_i (x/L)$
POSIT	x/L
T	$\sin(4\varphi_i^2 a^2/L^2)t$
TIME	t
VEL	v_{zo}
W	w
W1	$\frac{1}{\varphi_i^3}\left\{\frac{\sin(2\varphi_i x/L)/\cos\varphi_i - \sinh(2\varphi_i x/L)/\cosh\varphi_i}{(1/\cos^2\varphi_i) - (1/\cosh^2\varphi_i) + (2M/\varphi_i^2)}\right\}\sin\frac{4\varphi_i^2 a^2}{L^2}$
W2	$\sum_{i=1}^{7} W1$
XDEN	$\frac{1}{\cos^2\varphi_i} - \frac{1}{\cosh^2\varphi_i} + \frac{2M}{\varphi_i^2}$
XMASS	M
XNUM	$[\sin(2\varphi_i x/L)/\cos\varphi_i] - [\sinh(2\varphi_i x/L)/\cosh\varphi_i]$

TABLE IV

Test Beam Description

Material	Aluminum
E	10.04×10^6 psi
ν	0.294
L	52 inches
b	1.5 inches
h	0.25 inch
ρ	168.2 lb/ft^3

Note: Wide flange support beam not shown

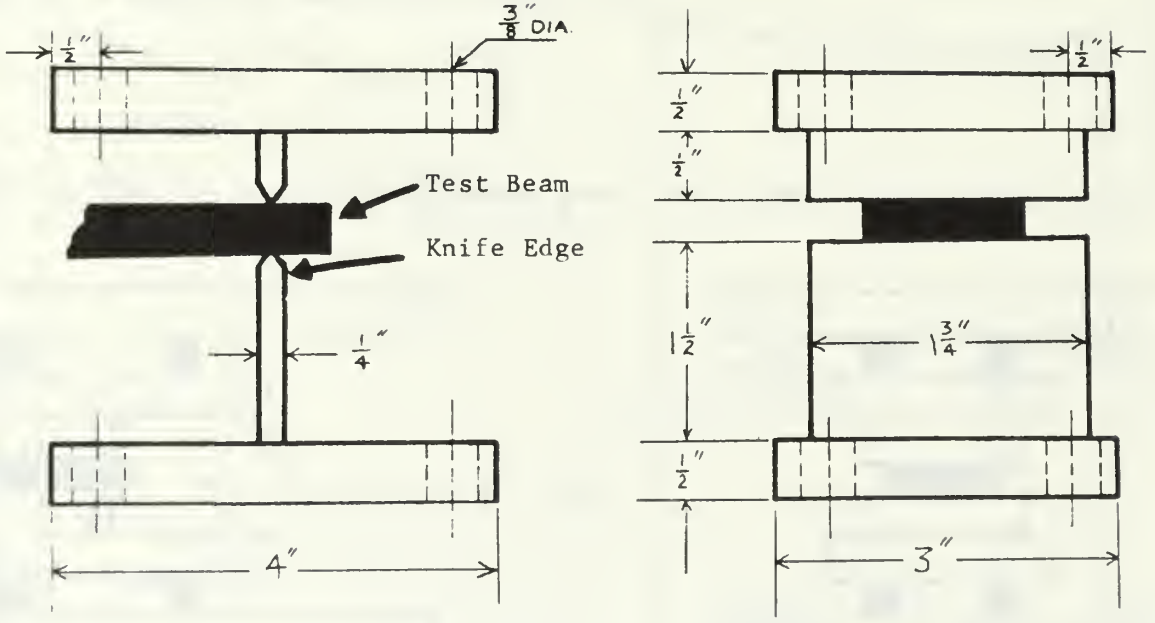

Figure 1. Diagram of Support at Pinned End of Test Rig

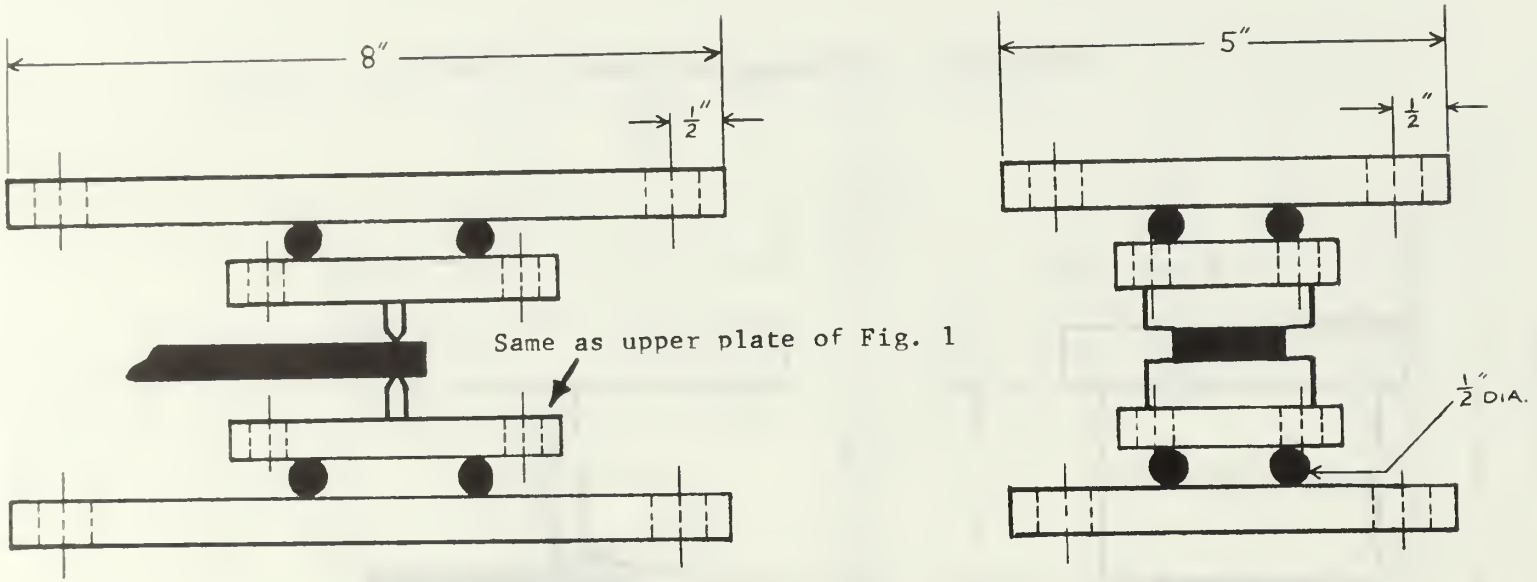

Note: Roller guides and wide flange support beam not shown

Figure 7. Diagram of Support at Moving End of Test Rig

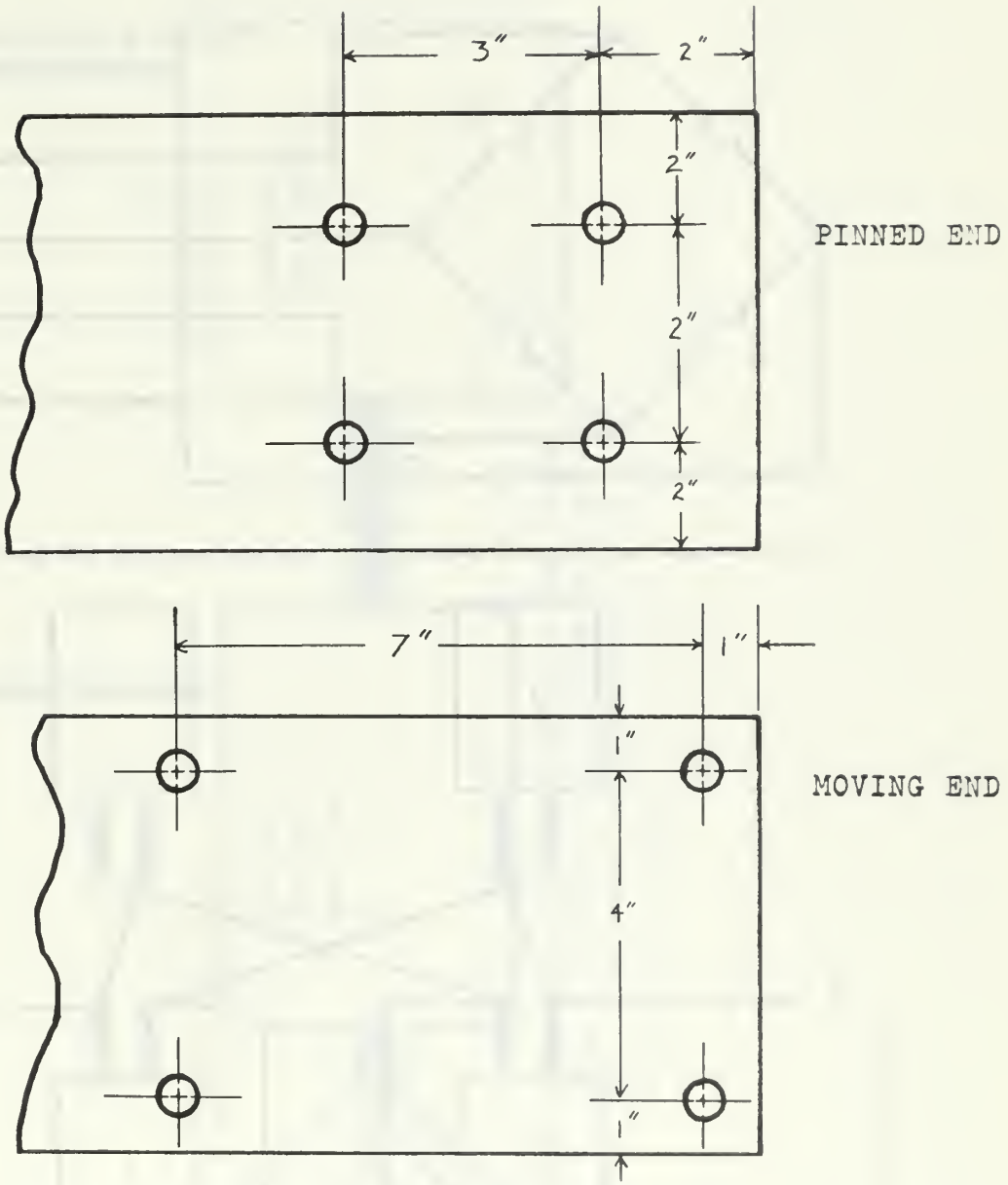

Note: Support beam is aluminum, 6" x 6" x 5'
Flange thickness = .25"

Figure 3. Diagram of Knife Edge Plate Locations on Support Beam

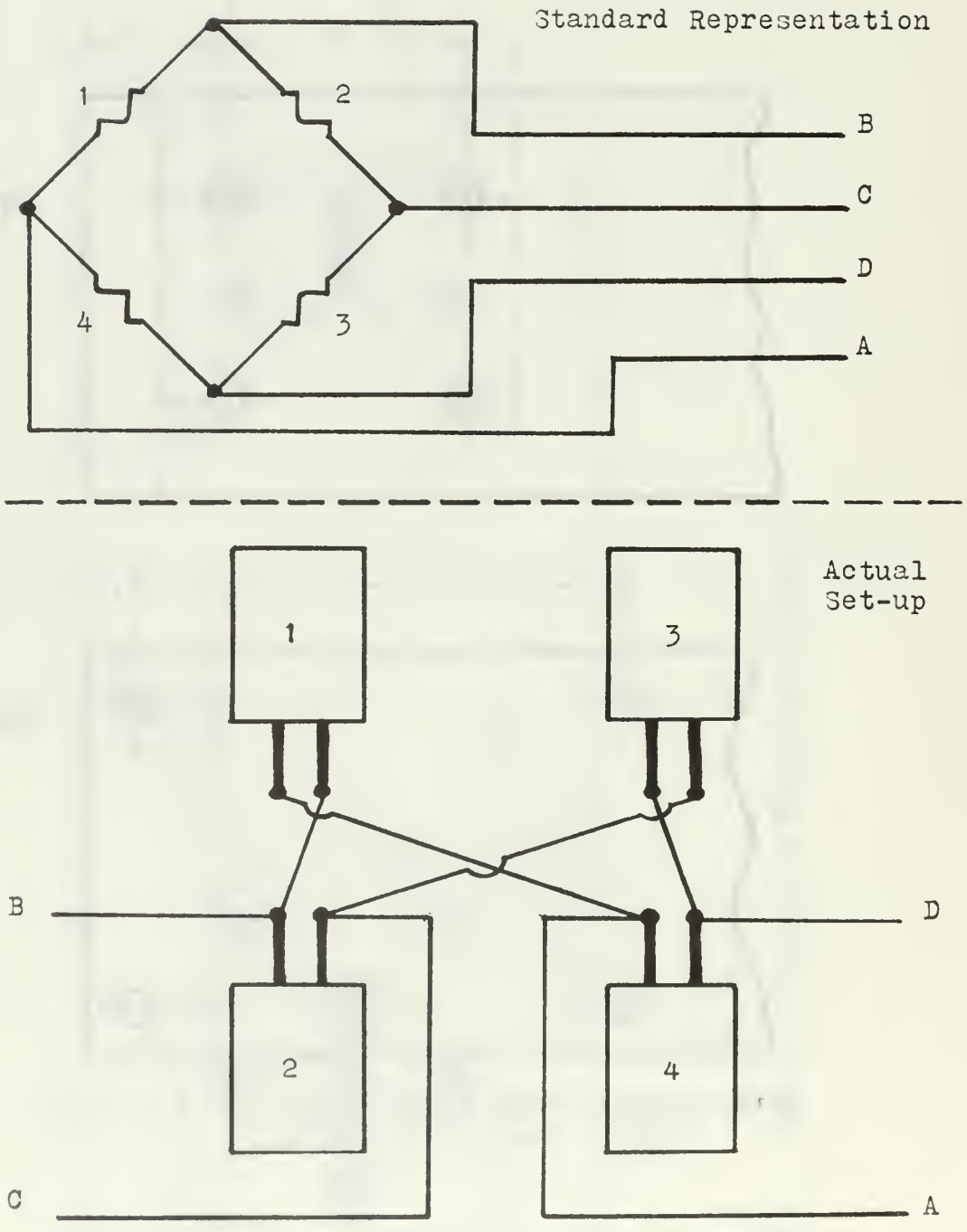

Note: Gages 1 and 3 active; 2 and 4 compensating

Figure 4. Bridge Wiring Diagram

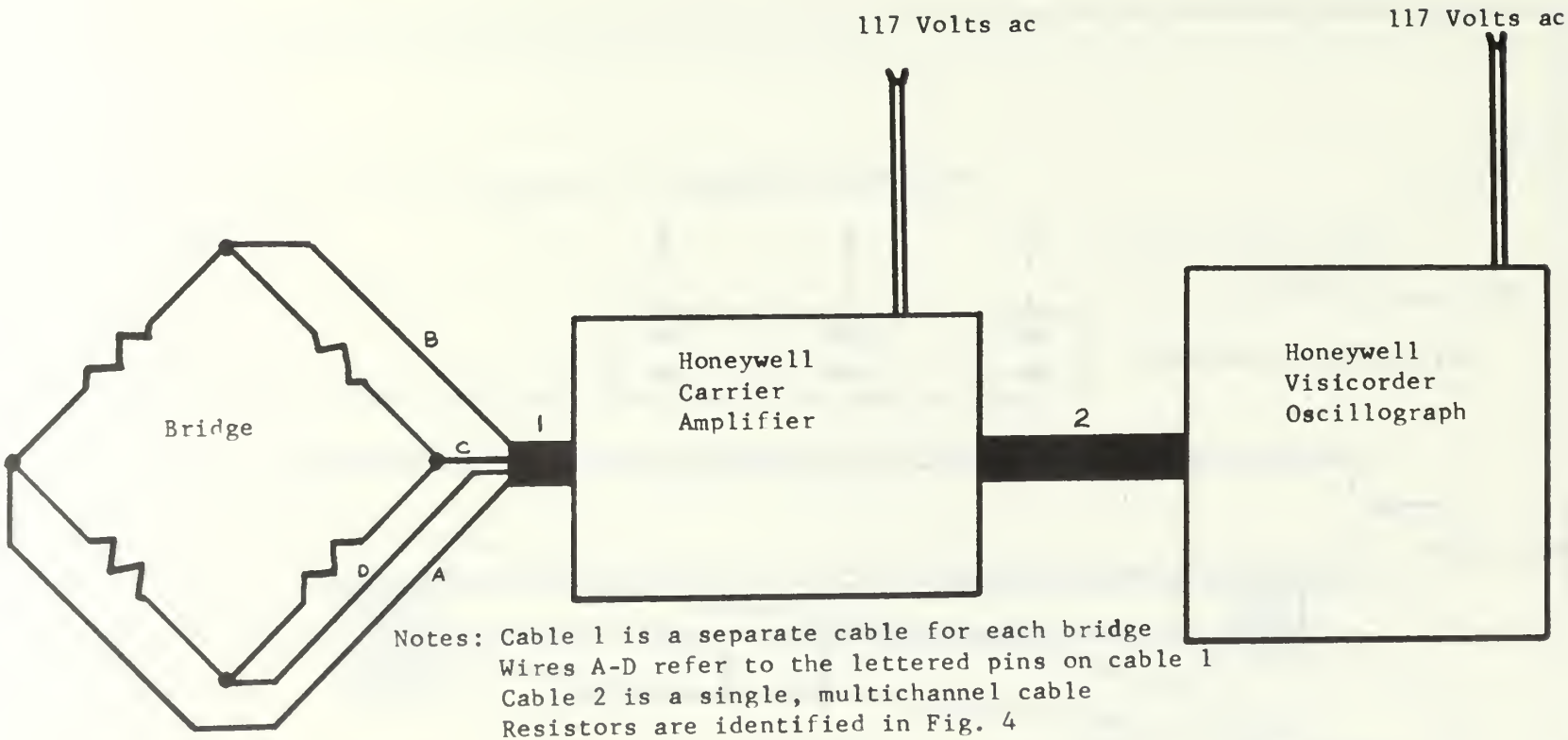

Notes: Cable 1 is a separate cable for each bridge
Wires A-D refer to the lettered pins on cable 1
Cable 2 is a single, multichannel cable
Resistors are identified in Fig. 4

Figure 5. Overall wiring Diagram

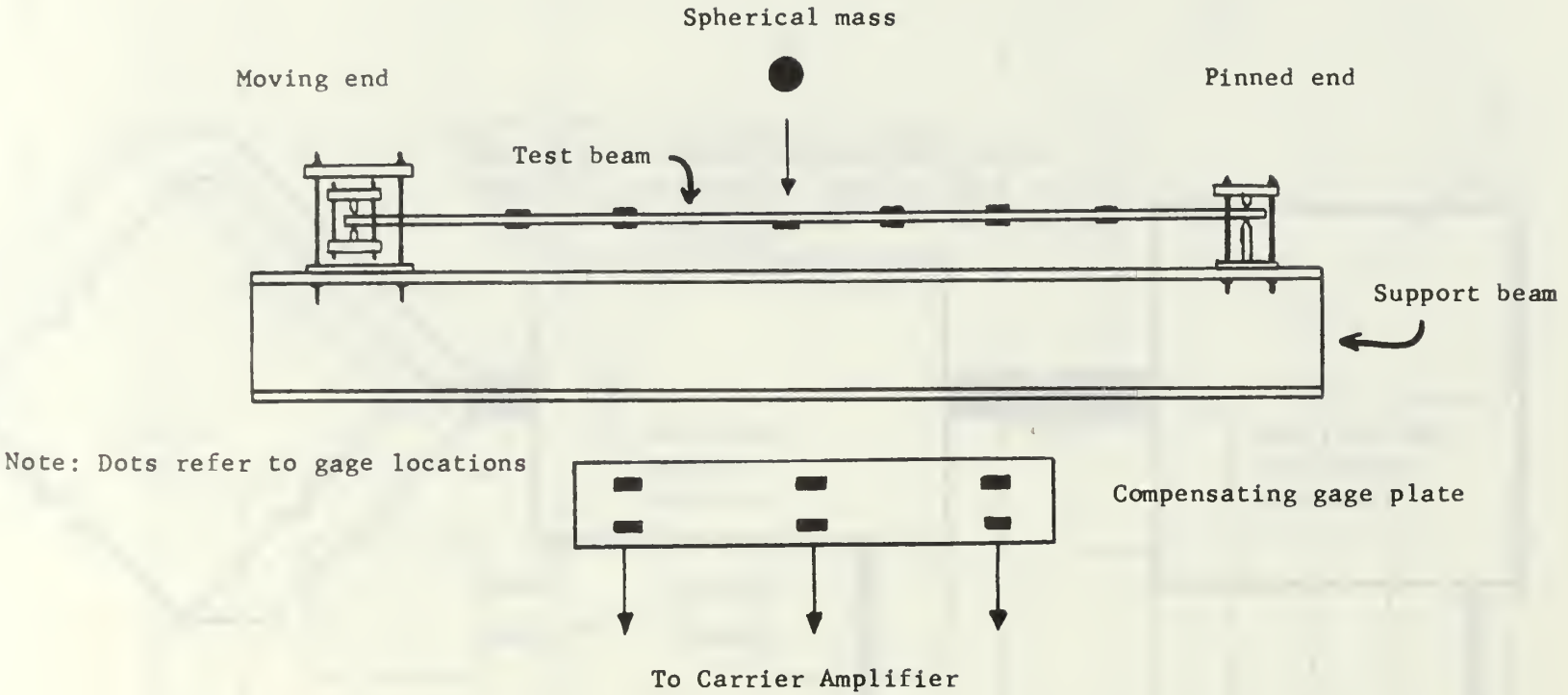

Figure 6. Diagram of Test Rig Assembly

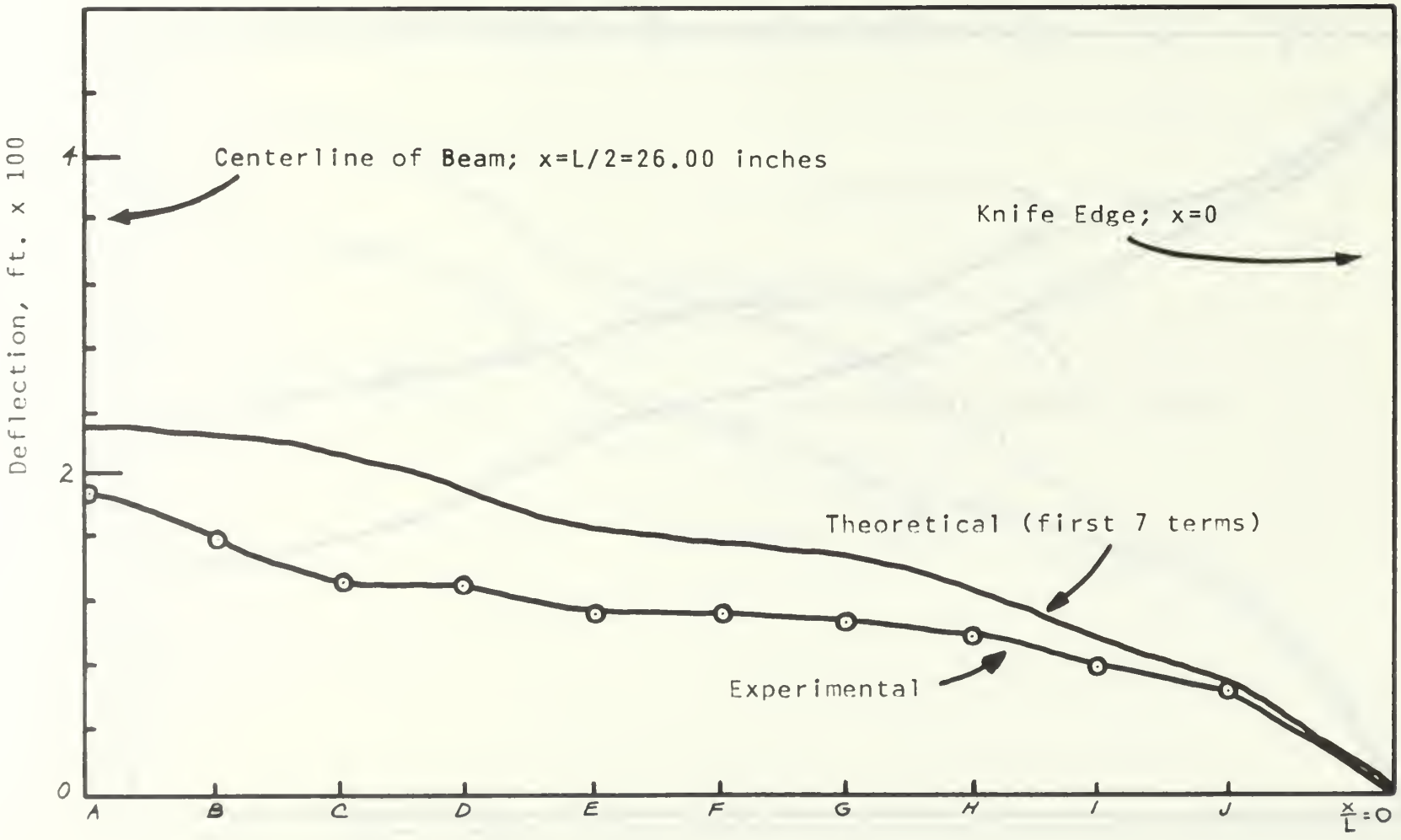

Figure 7. Maximum Deflection at Stations A through J for m_2 = 97.0 grams and v_{20} = 2.84 ft/sec

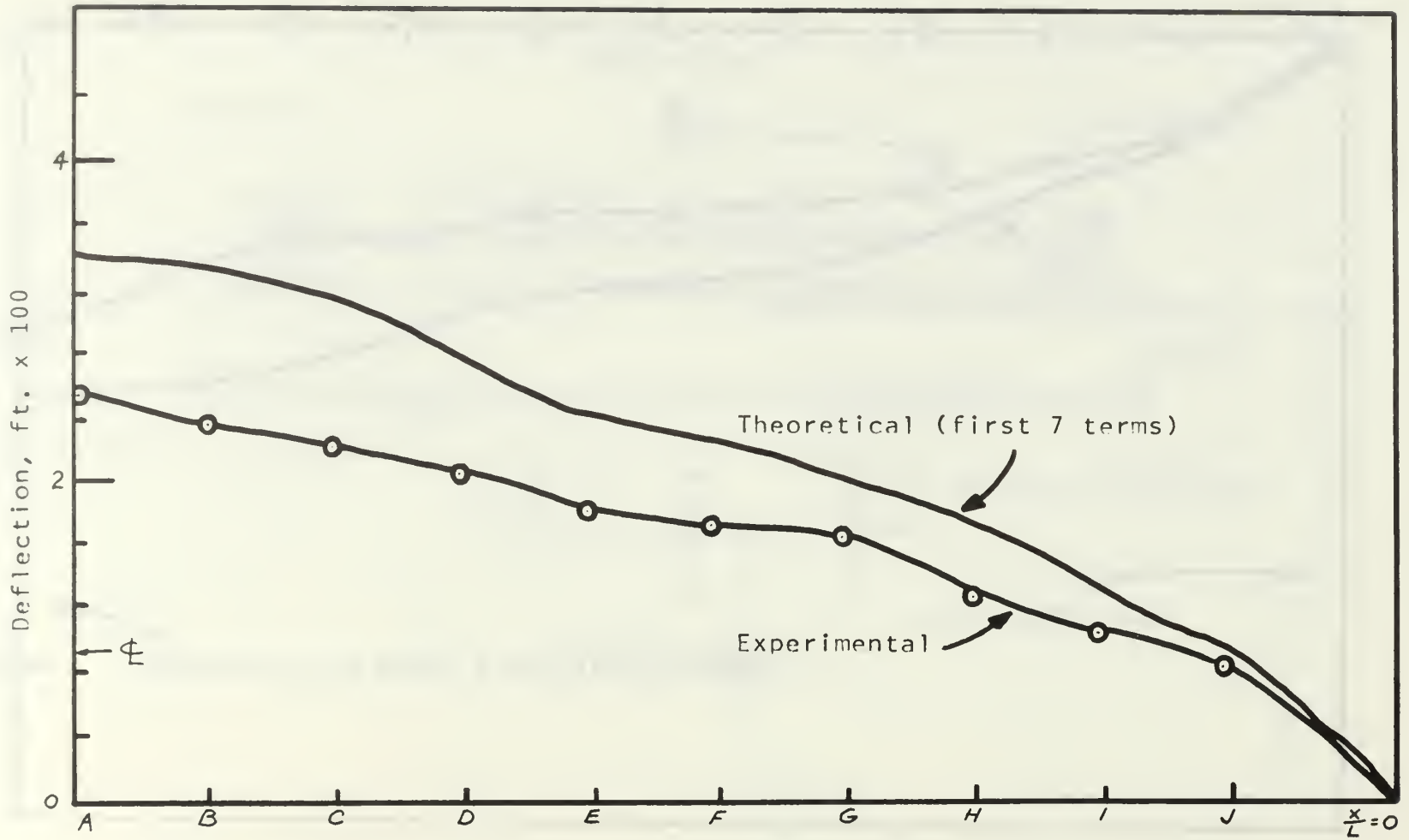

Figure 8. Maximum Deflection at Stations A through J for m_2 = 97.0 grams and v_{20} = 4.02 ft/sec

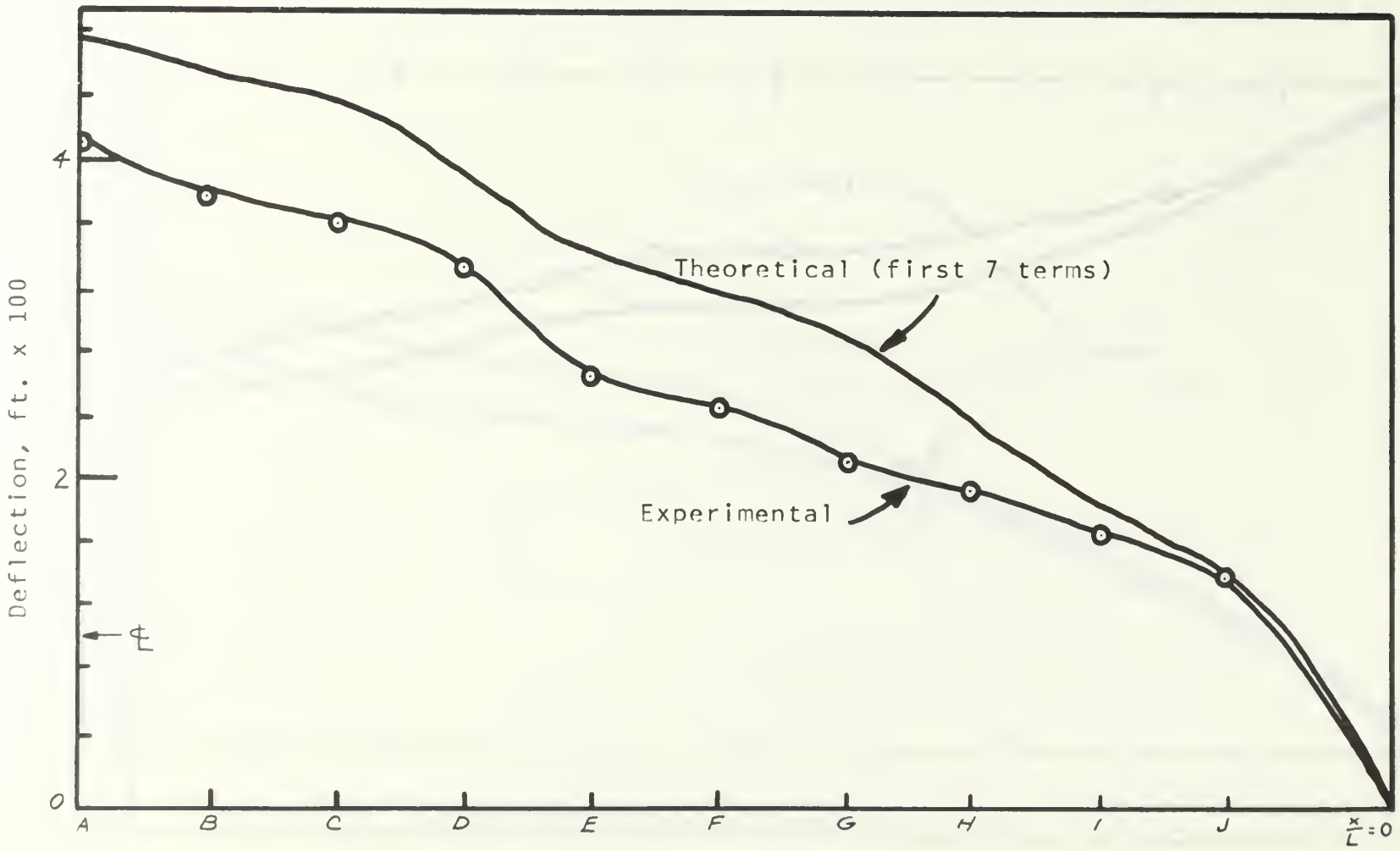

Figure 9. Maximum Deflection at Stations A through J for m_2 = 97.0 grams and v_{20} = 5.68 ft/sec

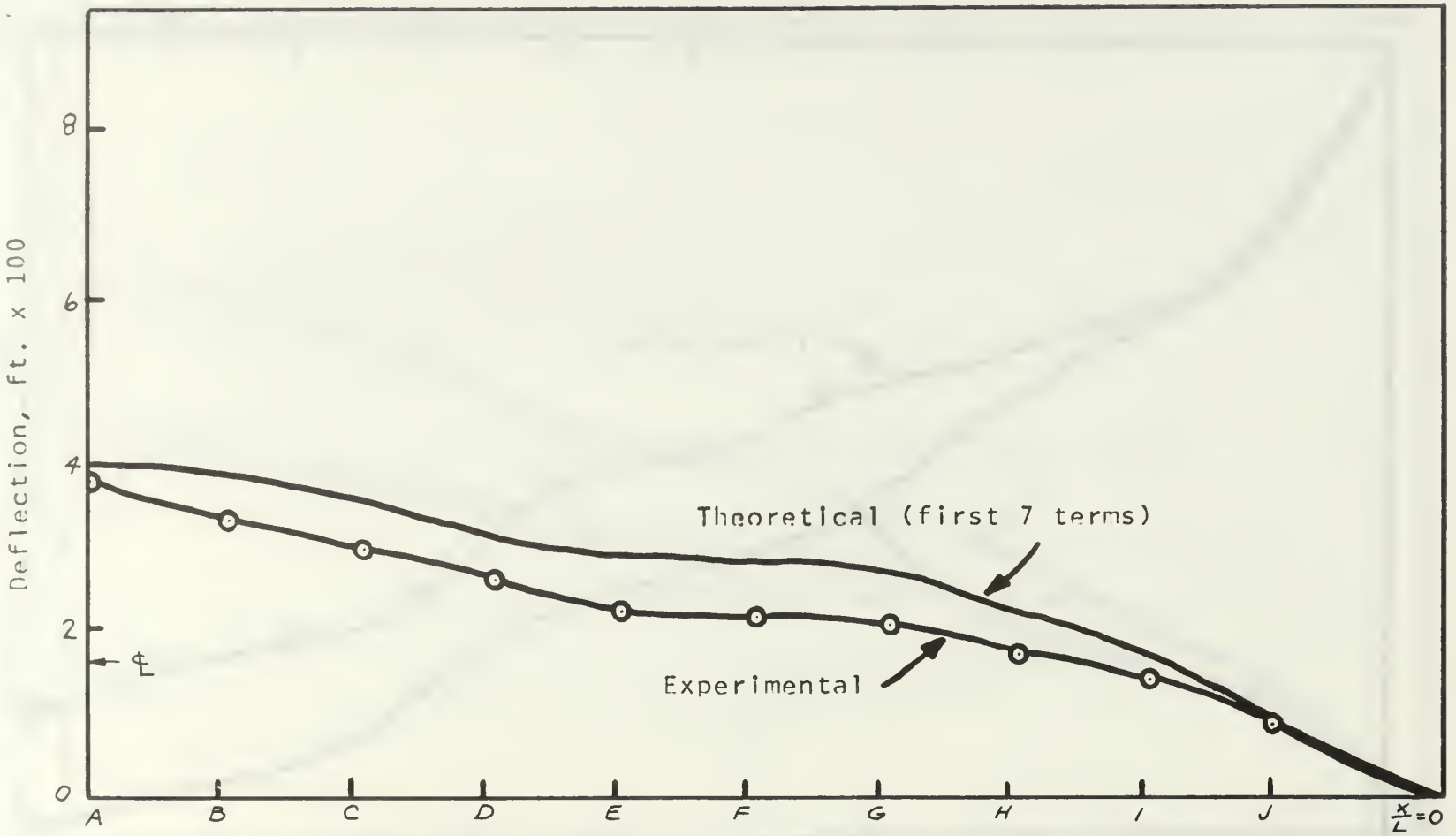

Figure 10. Maximum Deflection at Stations A through J for m_2 = 493.5 grams and v_{20} = 2.84 ft/sec

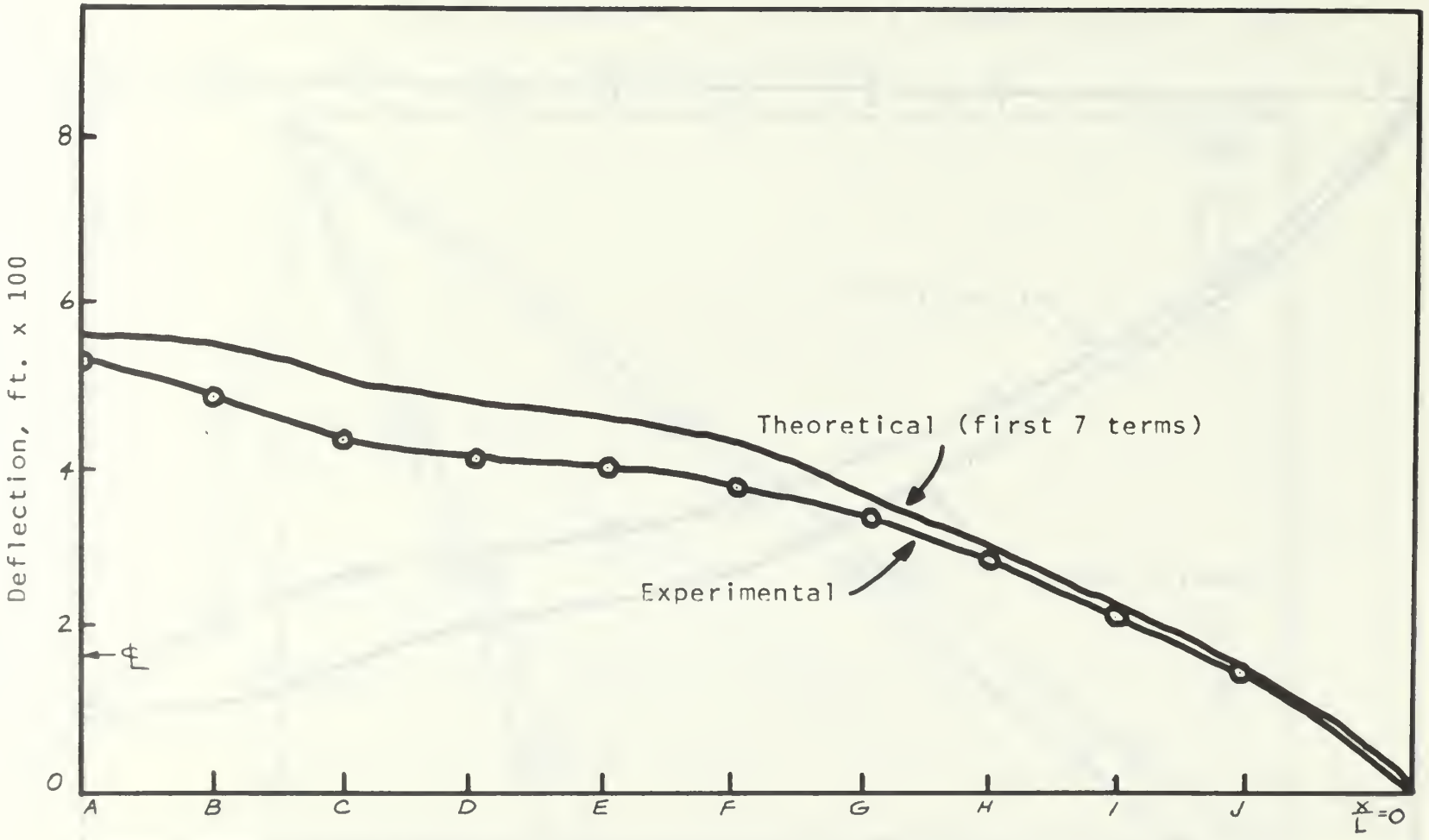

Figure 11. Maximum Deflection at Stations A through J for m_2 = 493.5 grams and v_{20} = 4.02 ft/sec

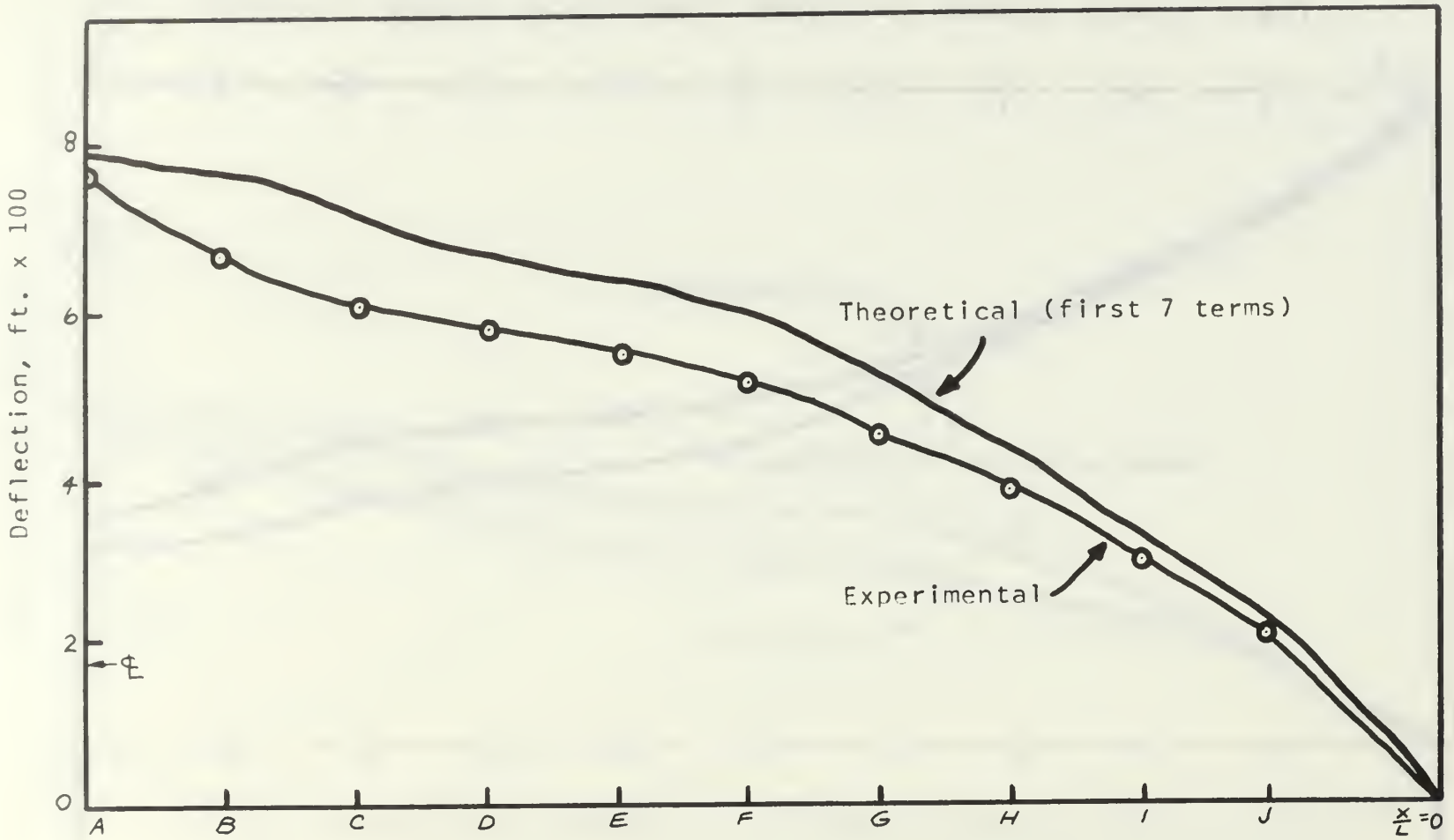

Figure 12. Maximum Deflection at Stations A through J for m_2 = 493.5 grams and v_{20} = 5.68 ft/sec

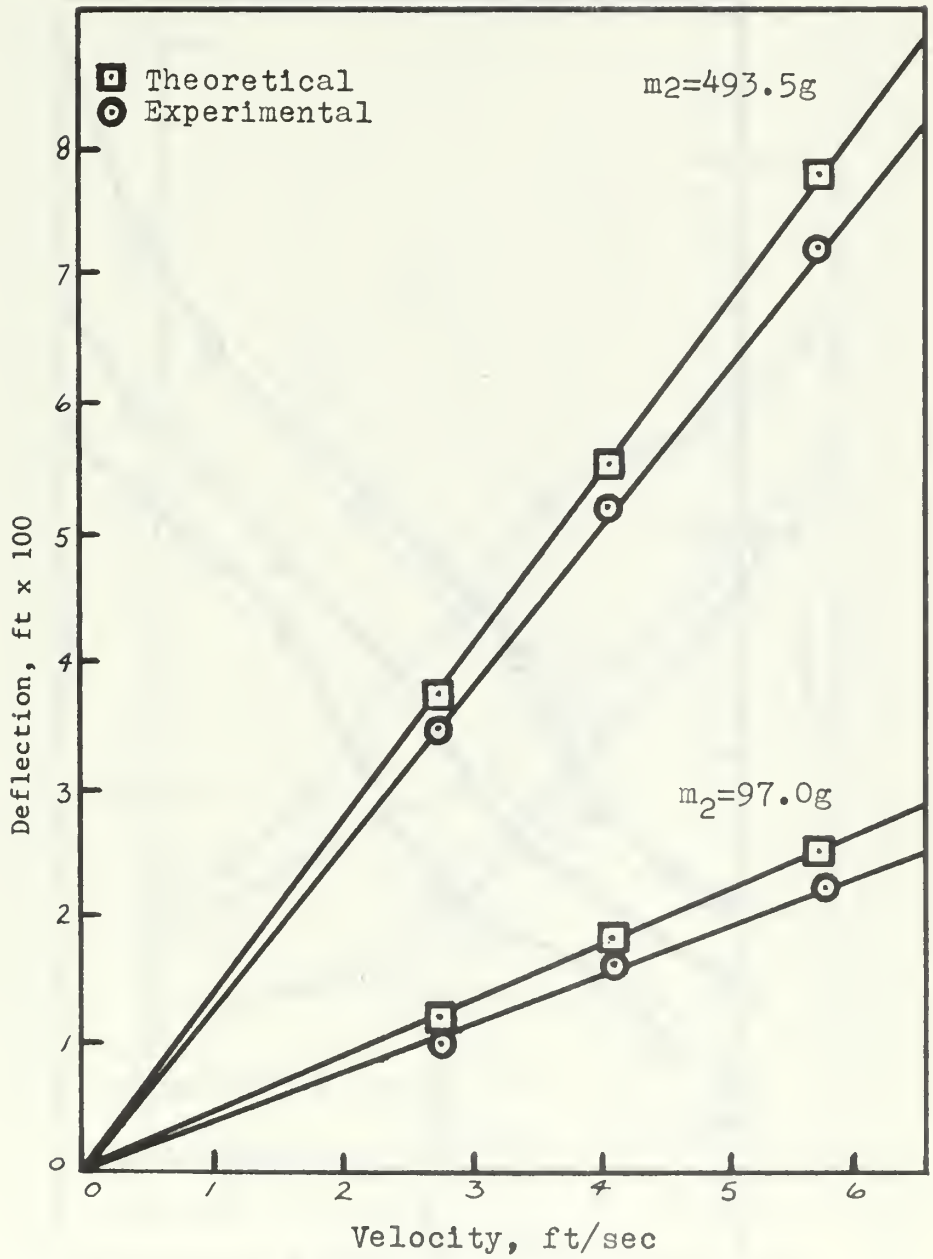

Figure 13. Maximum Deflection at x/L = .5000 vs. Various Velocities of m_2 at Impact

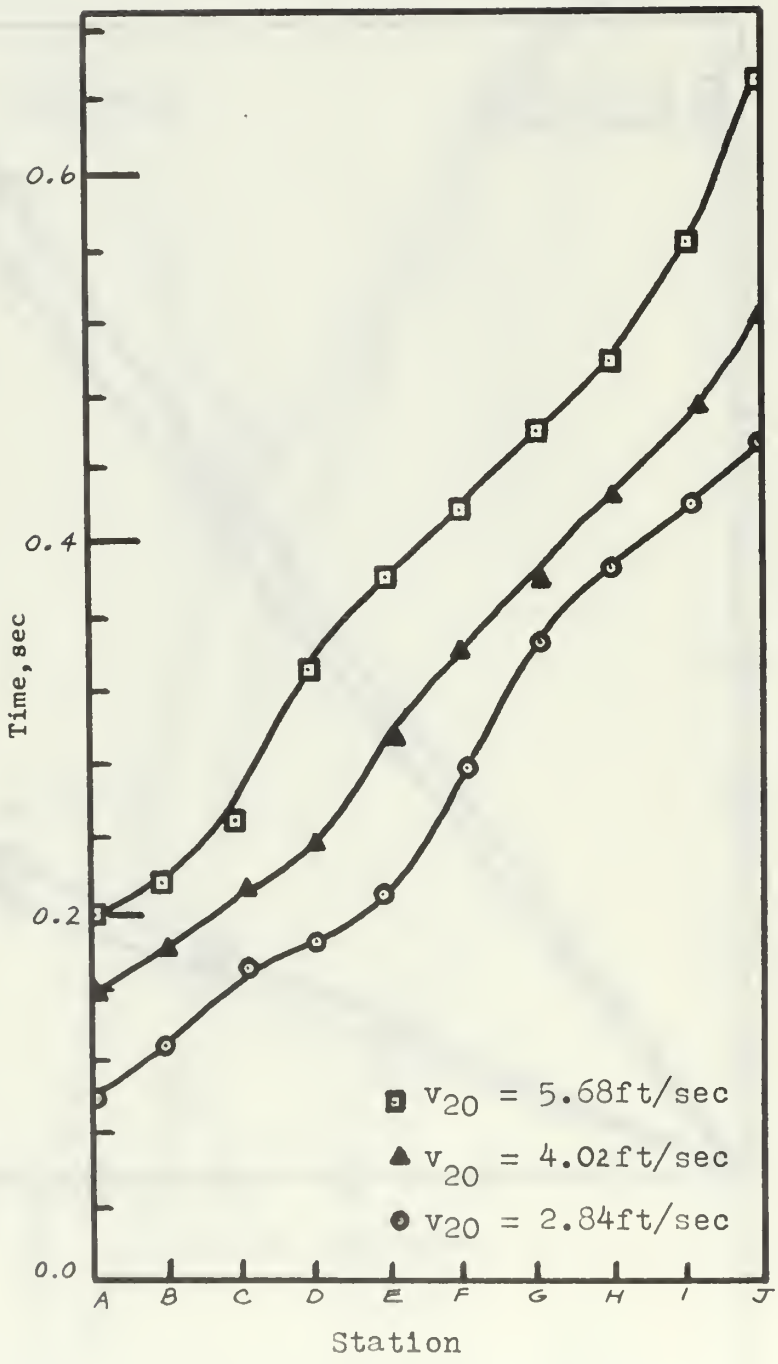

Figure 14. Decay Time of Higher Order Frequencies at Stations A through J for m_2 = 97.0g

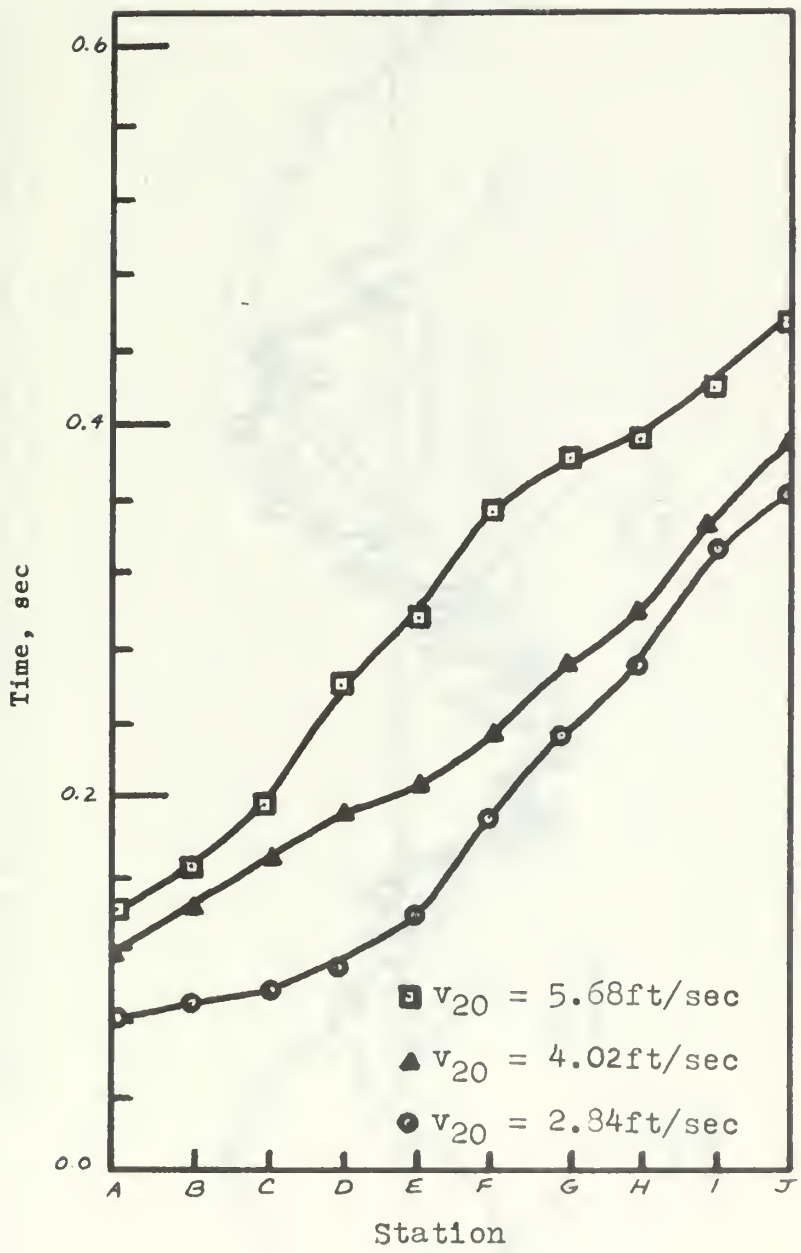

Figure 15. Decay Time of Higher Order Frequencies at Stations A through J for m_2 = 493.5g

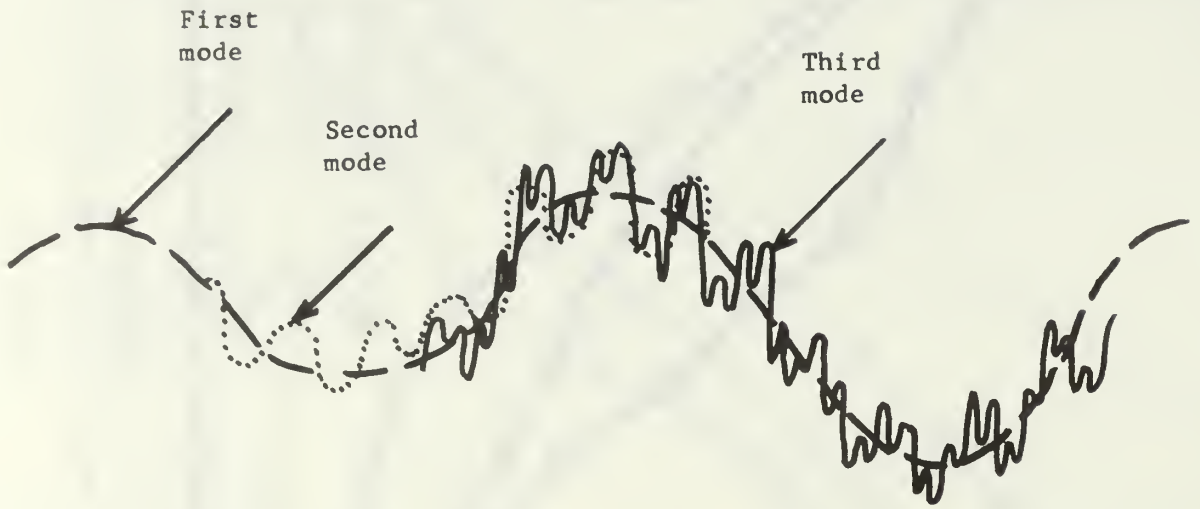

Figure 16. Distinction of Modes of Vibration from Visicorder Oscillograph Output

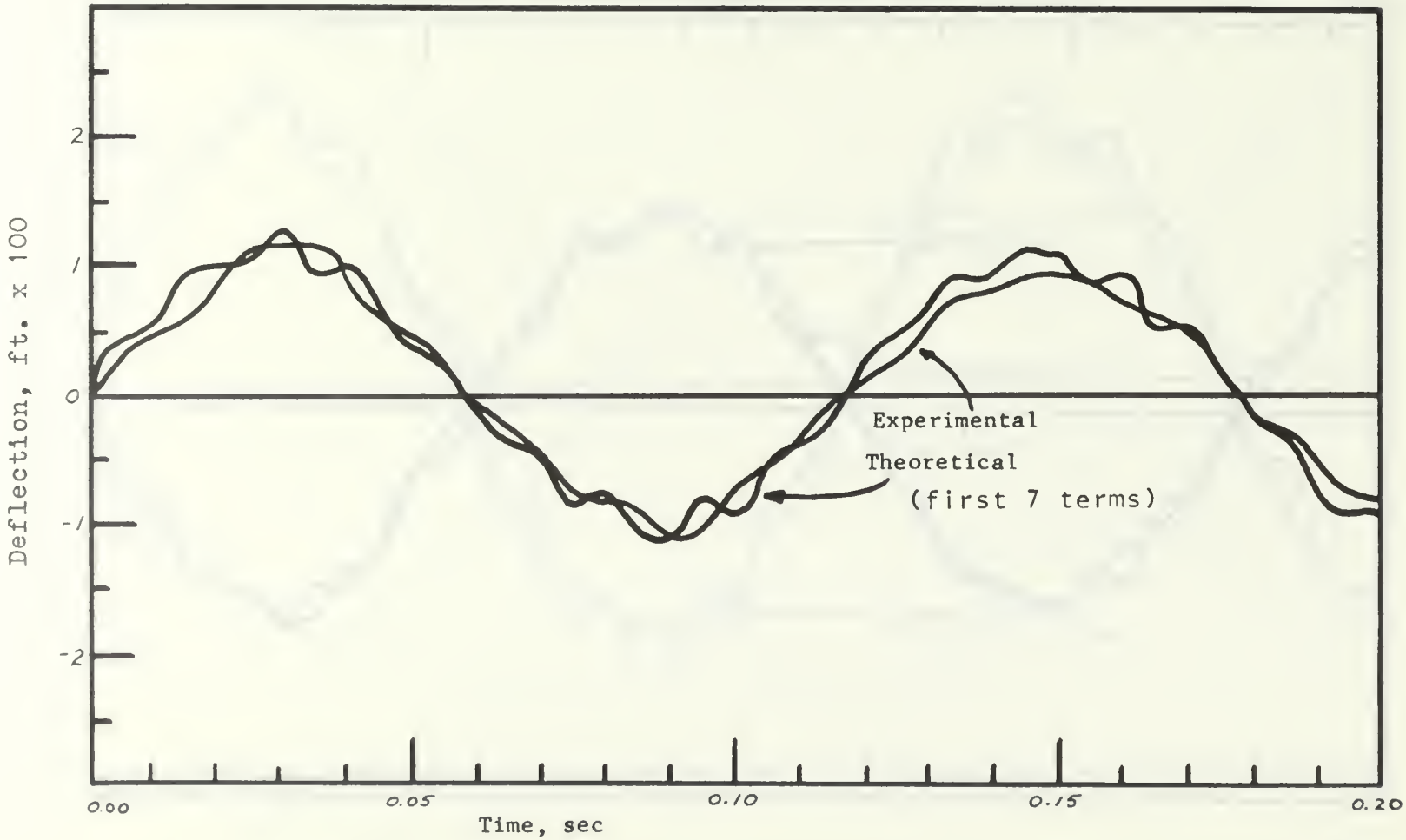

Figure 17. Displacement vs. Time at x/L = .5000 for m_2 = 97.0 grams and v_{20} = 2.84 ft/sec

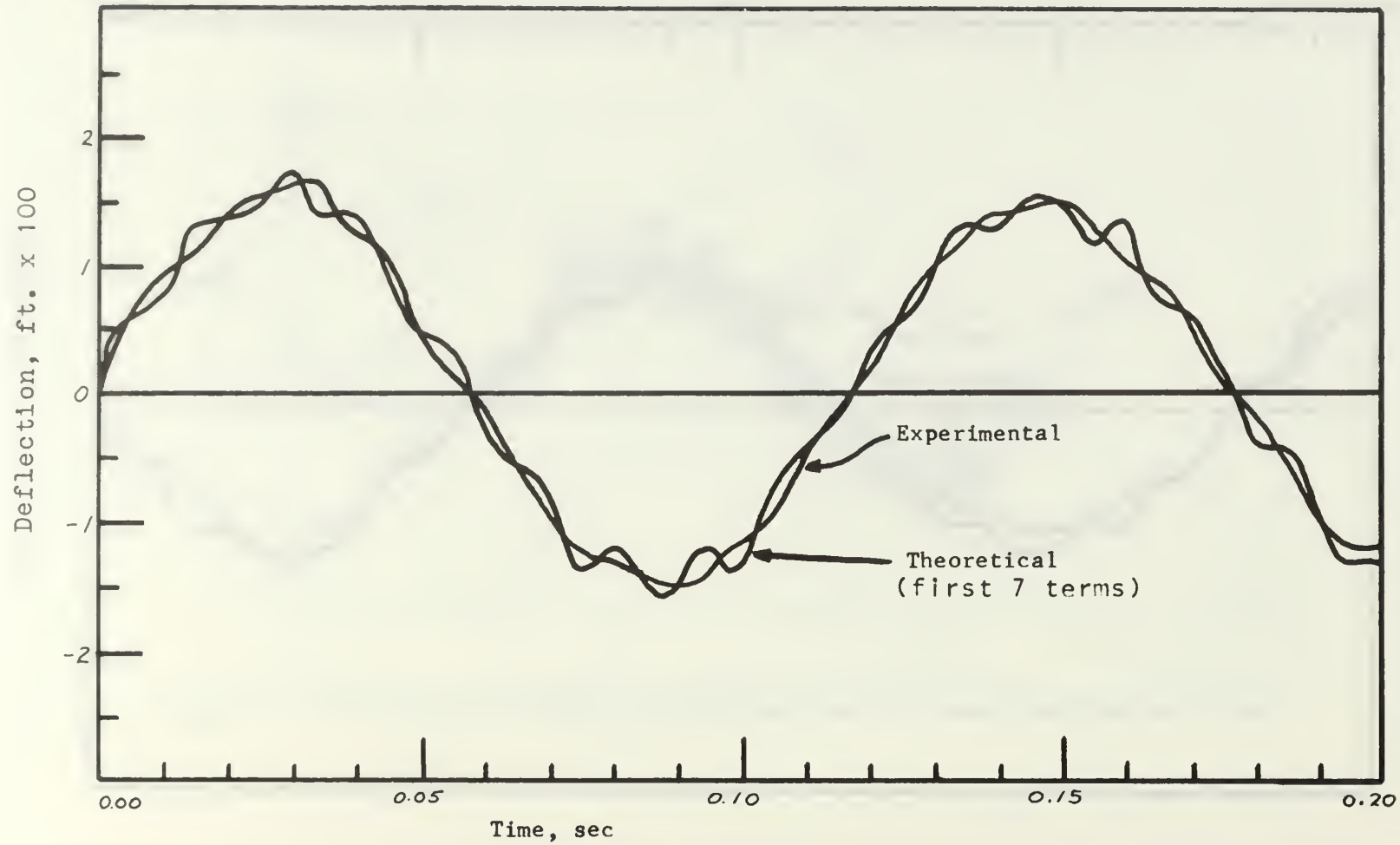

Figure 18. Displacement vs. Time at x/L = .5000 for m_2 = 97.0 grams and v_{20} = 4.02 ft/sec

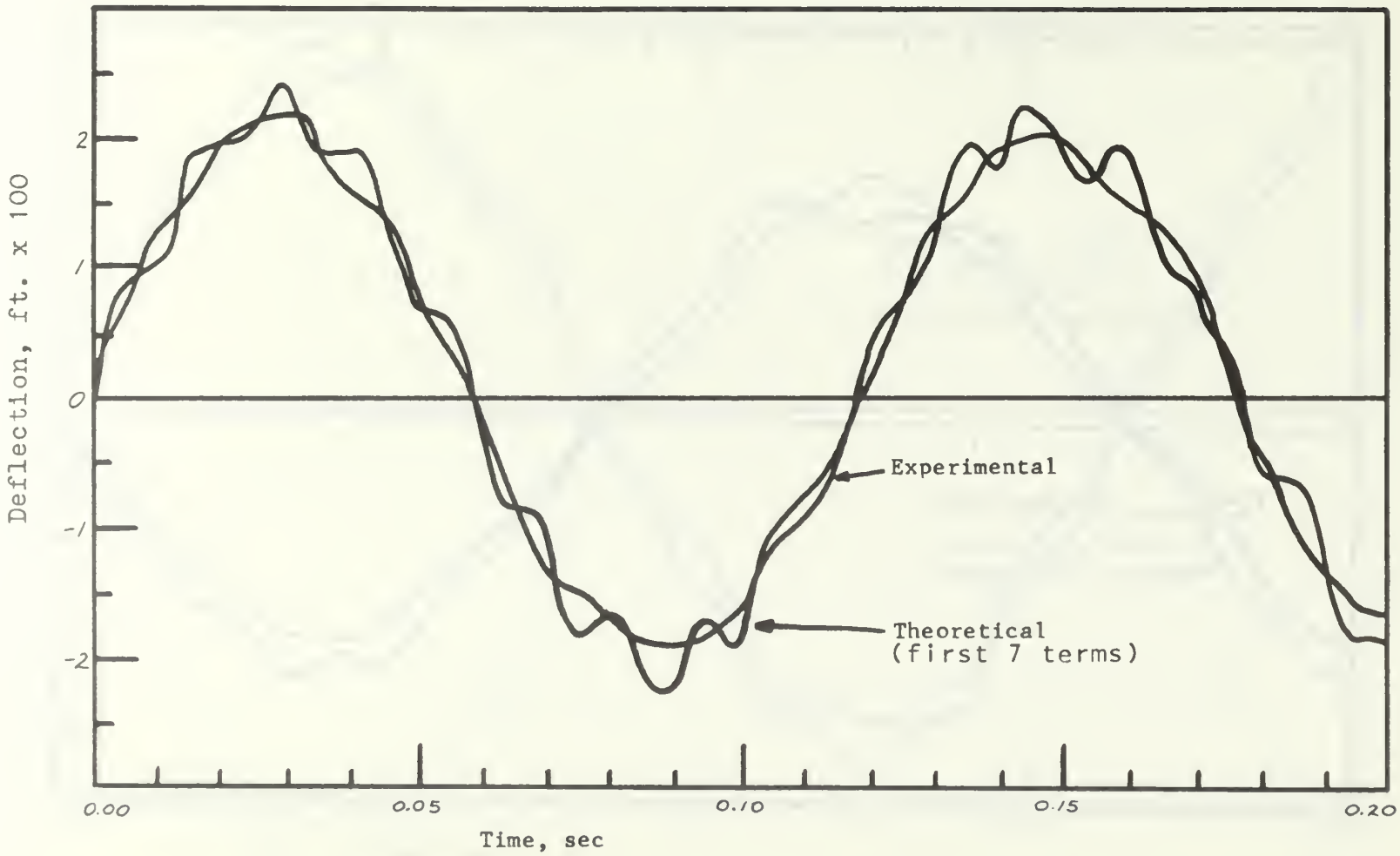

Figure 19. Displacement vs. Time at x/L = .5000 for m_2 = 97.0 grams and v_{20} = 5.68 ft/sec

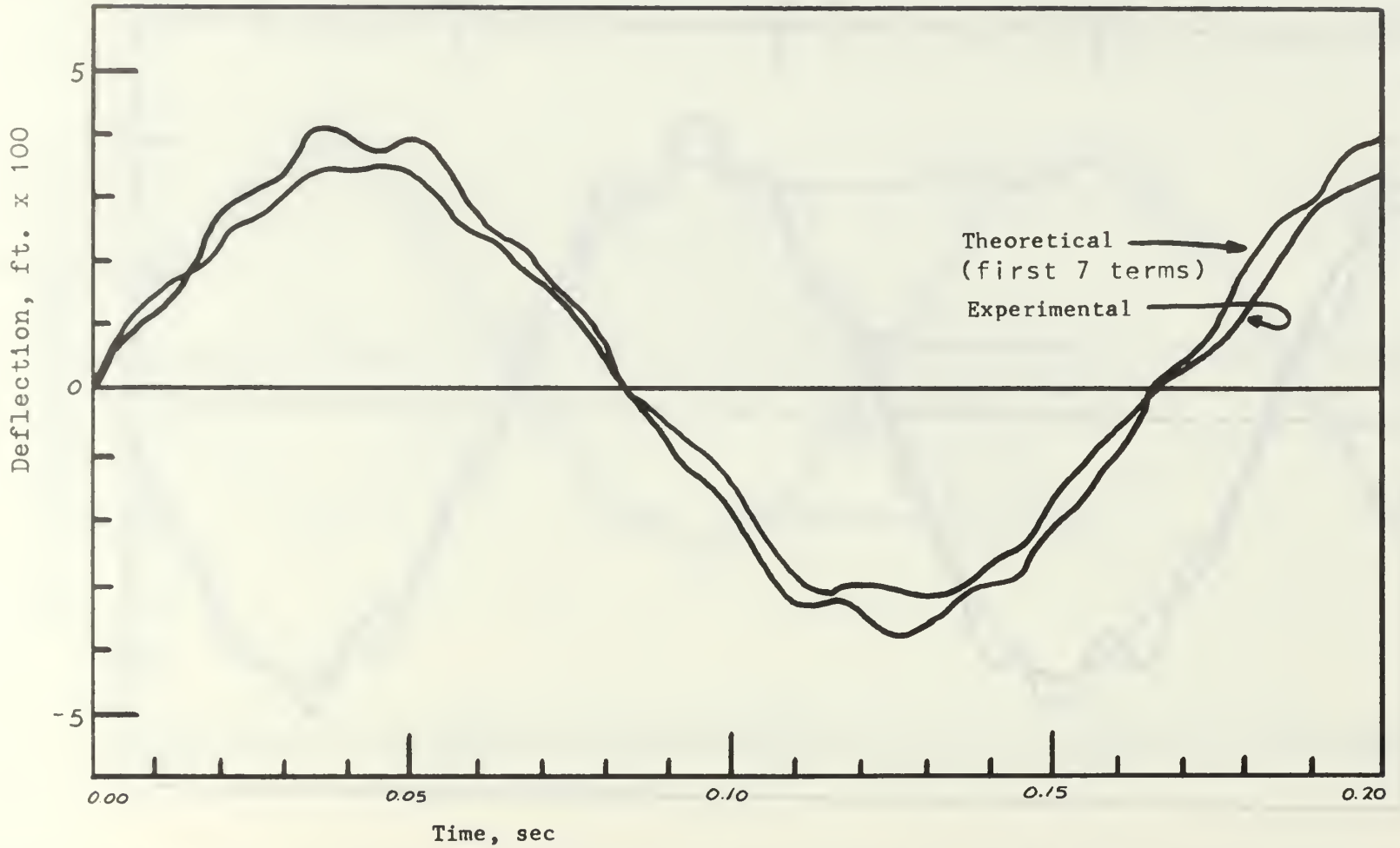

Figure 20. Displacement vs. Time at x/L = .5000 for m_2 = 493.5 grams and v_{20} = 2.84 ft/sec

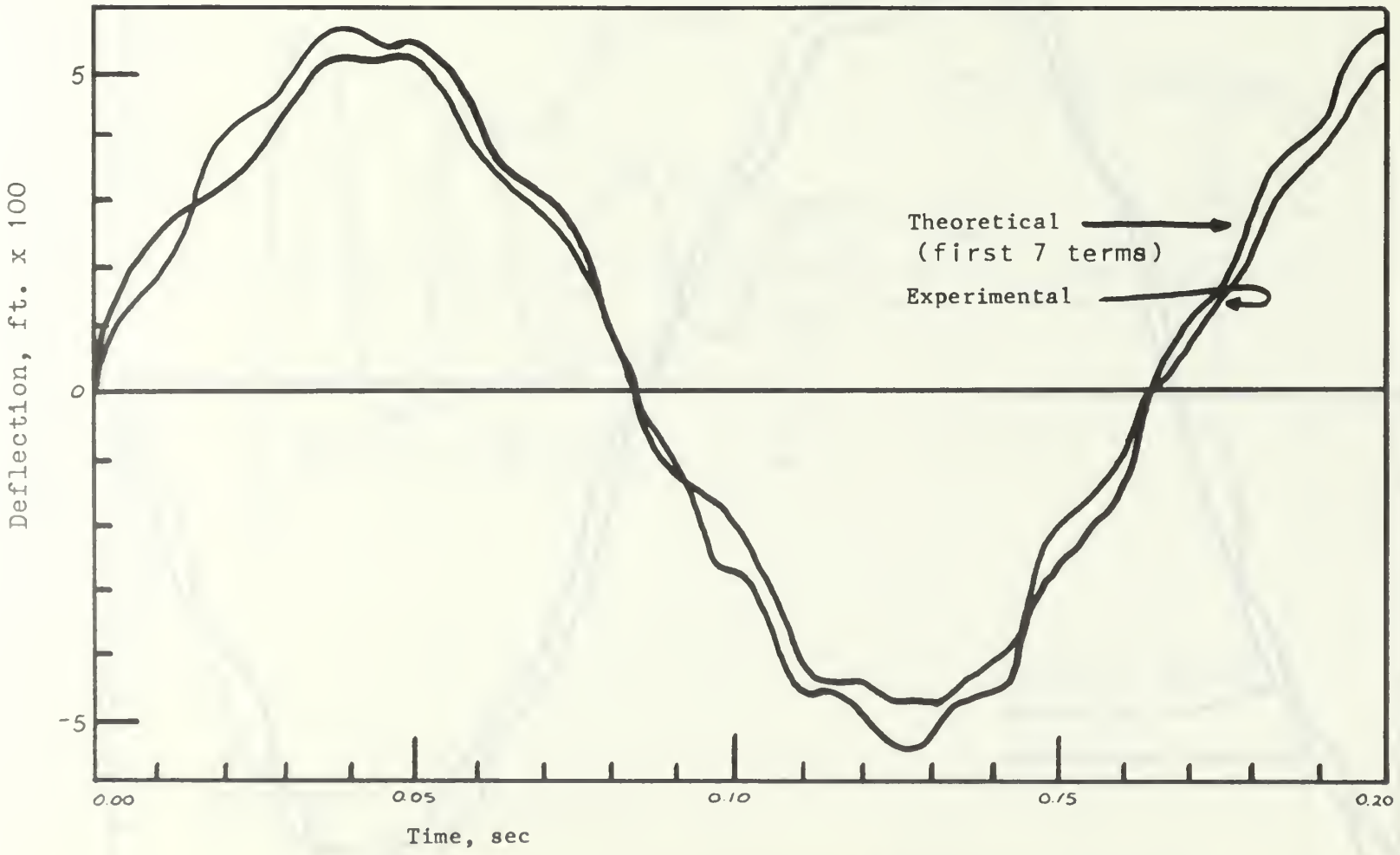

Figure 21. Displacement vs. Time at x/L = .5000 for m_2 = 493.5 grams and v_{20} = 4.02 ft/sec

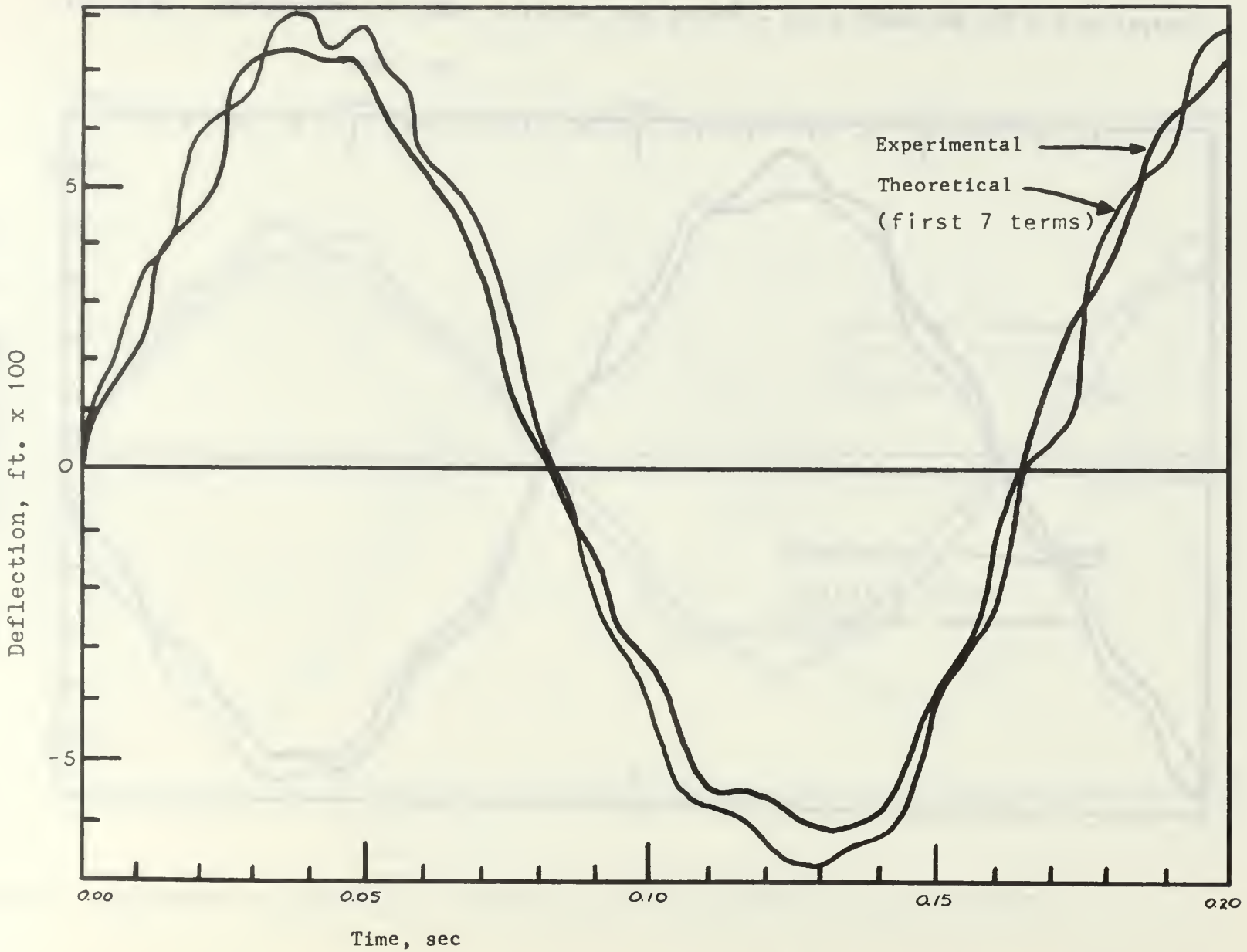

Figure 22. Displacement vs. Time at x/L = .5000 for m_2 = 493.5 grams and v_{20} = 5.68 ft/sec

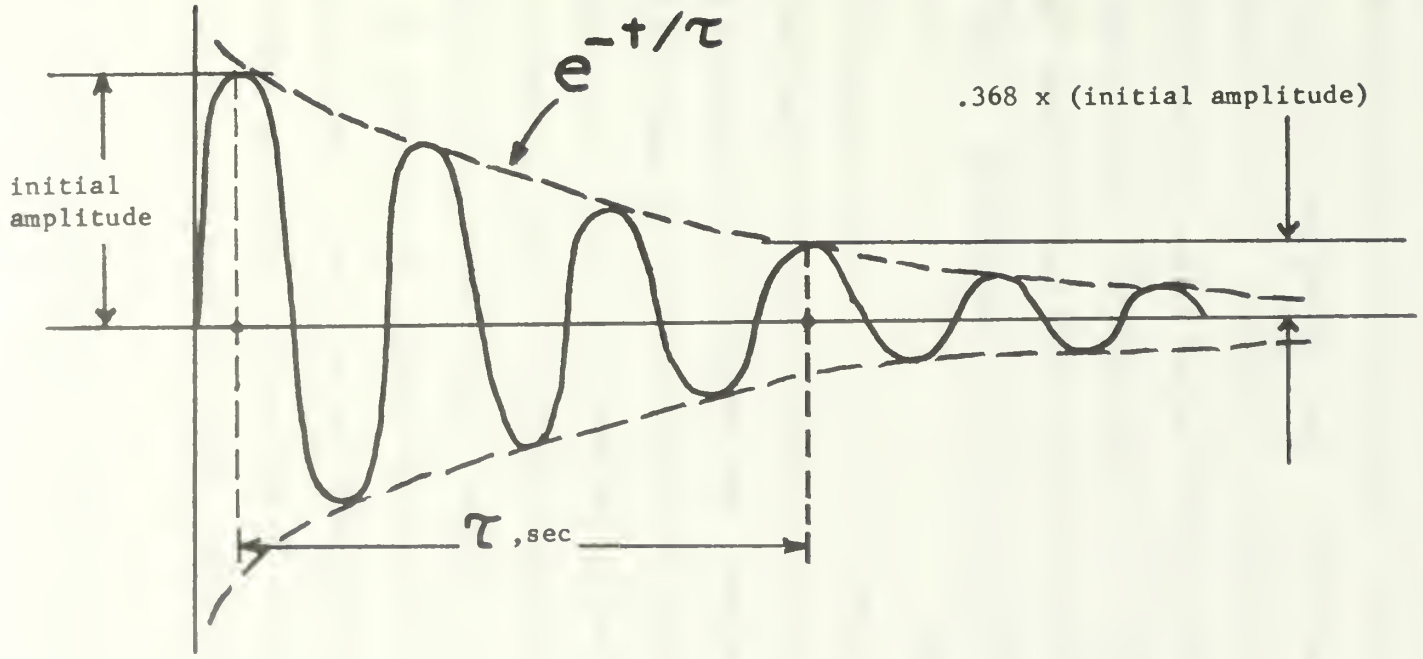

Figure 23. Determination of Decay Constant

APPENDIX A STRAIN GAGE TECHNIQUES

The strain gages which were used were described in the section "DESCRIPTION OF EQUIPMENT". They were all from lot number 232-1. The gages were wire gages with a paper backing and a protective felt pad on the top. After application, they were cured for a period of thirty hours with a flat two-pound weight (separated from the gages by foam rubber) to prevent the formation of air bubbles between the beam and the gage backing. The cement used was SR-4 Strain Gage Cement, manufactured by the Baldwin-Lima-Hamilton Corporation. It was similar to ordinary Duco cement.

After all of the gages had been cured, it was necessary to check for air bubbles. This was done by tapping the top of the gage while applying no stress to the beam. Had the gage not been properly cemented to the beam, the air space would have permitted the gage wire to deform, and hence a deflection would have been noticed on a strain indicator.

Certain steps were taken in wiring the bridges to allow for the displacement of the active gages. Copper connectors with non-conducting backings were cemented to the test beam near the lead wires of the various gages. Longer wires were then led from the connectors to the plate holding the compensating gages so that, should any soldered connections be accidentally jarred loose, the break would not affect the gages themselves.

These longer wires were shaped to provide flex loops to allow for the changing distance between the points that they connected.

Compensating gages were affixed to a slab of aluminum identical to the test beam material. The compensating gages were used to avoid false

strain indications due to temperature changes. The false indications may arise from two factors. First, the electrical resistance of most conductors changes with temperature. A second temperature effect occurs if the thermal coefficient of expansion of the strain gage filament is different from that of the structure to which it is bonded. Because the test beam and the slab to which the compensating gages were affixed were subjected to the same temperatures during testing, both active and compensating gages experienced identical thermal resistance changes. This was true whether resistance changes occurred due to the temperature coefficient of electrical resistance or to the differential expansion existing between the gages and the metal to which they were bonded.

APPENDIX B CALCULATION OF TEST BEAM PROPERTIES

The method of obtaining the modulus of elasticity and Poisson's ratio for a test specimen cut from the test beam is referred to in the section, "EXPERIMENTAL PROCEDURE". The incremental moment loading test yielded the following data:

Weight Nos.	M_B	ΔM_B	ϵ_x	$\Delta\epsilon_x$	ϵ_z	$\Delta\epsilon_z$
(none)	0		0		0	
		54.99		340		100
1,2	54.99		340		100	
		55.05		340		100
1-4	110.04		680		200	
		55.08		340		100
1-6	165.12		1020		300	

The values of the weights (pounds) were:

Weight No.	W
1	5.499
2	5.499
3	5.499
4	5.510
5	5.499
6	5.515

The bending jig was such that the moment arm had a length of ten inches and the specimen length was twelve inches. The units of M_B were in-lb, of ϵ , μ in/in, and the specimen dimensions inches.

From the flexure formula, the following relationship is obtained:

$$E = [M_B (h/2)] / [\epsilon_{x_{max}} I] \quad . \qquad (25)$$

This becomes:

$$E = \frac{M_B(h/2)}{\epsilon_{x\,max}(bh^3/12)} \tag{26}$$

For the three increments of loading, the value of E was found to be $E = 10.04 \times 10^6$ psi.

At a glance, from $\nu = \Delta\epsilon_z / \Delta\epsilon_x$, the value of ν (27) was found to be $\nu = 0.294$.

The density ρ for the specimen was calculated using the relationship

$$\rho = m_t / \mathcal{V} \quad . \tag{28}$$

The specimen had the dimensions 11.75x1.5x0.25 in^3. The mass of the specimen, using the Ohaus balance, was 194.5g. Upon substitution of the proper values, $\rho = 168.2$ lbm/ft^3.

For purposes of comparison, the "book" values of the properties discussed are:

$$E = 9.5 \text{ to } 10.5 \times 10^6 \text{ psi}$$

$$\nu = 0.3 \text{ to } 0.33$$

$$\rho = 168.2 \text{ lbm/ft}^3$$

COMPUTER SOLUTION OF EQUATION (24)

DISPLACEMENT OF A UNIFORM BEAM UNDER IMPACT LOADING

```
      DIMENSION FI(7),VEL(3),POSIT(10)
      READ(5,10) (FI(I),I=1,7)
      READ(5,11) (VEL(J),J=1,3)
      READ(5,12) (POSIT(K),K=1,10)
   10 FORMAT (7F10.3)
   11 FORMAT (3F10.3)
   12 FORMAT (10F6.5)
      WRITE (6,102)
  102 FORMAT (1H1)
      WRITE (6,101)
      XMASS=1.73
      TIME=0.0
      GO TO 20
   30 XMASS=8.8
      READ(5,10) (FI(I),I=1,7)
      TIME=0.0
   20 DO 60 J=1,3
      DO 40 K=1,10
      TIME=0.0
      DO 80 L=1,40
      TIME=TIME+.005
      W2=0.0
      DO 50 I=1,7
      FIXL=2.0*FI(I)*POSIT(K)
      XNUM=((SIN(FIXL)/COS(FI(I)))-SINH(FIXL)/COSH(FI(I)))
      XDEN=(1./(ABS(COS(FI(I)))))**2.0-(1./COSH(FI(I)))
     1**2.0+(2.0*XMASS/(FI(I))**2.)
      T=((4.*((FI(I)))**2.0)/.1845)*TIME
      W1=((1./FI(I))**3.0)*(XNUM/XDEN)*SIN(T)
      W2=W2+W1
   50 CONTINUE
      W=.1845*VEL(J)*W2
      WRITE (6,100) XMASS,W,POSIT(K),VEL(J),TIME
   80 CONTINUE
   40 CONTINUE
   60 CONTINUE
      IF(XMASS-5.0)30,30,70
  101 FORMAT(///,10X,'MASS',9X,'DISPLACEMENT',8X,'POSIT',
     111X,'VELOCITY',10X,'TIME')
  100 FORMAT(/,10X,F5.2,10X,F11.8,10X,F6.4,10X,F10.3,10X,
     1F6.4,/)
   70 STOP
      END
```

DATA CARDS:

FI(I) FOR M=1.73
VELOCITIES OF STRIKER AT IMPACT
VALUES OF X/L
FI(I) FOR M=8.80

TERMS USED ARE DEFINED IN TABLE III
THIS PROGRAM IS FOR THE FIRST SEVEN TERMS
OF THE INFINITE SUMMATION

BIBLIOGRAPHY

1. Arnold, R. N., Impact Stresses on a Freely Supported Beam. Proceedings of the Institution of Mechanical Engineers, v. 137, 1937.

2. Dally, J. W. and Riley, W. F., Experimental Stress Analysis. McGraw-Hill Book Company, Inc., 1965.

3. Dove, R. C. and Adams, P. H., Experimental Stress Analysis and Motion Measurement. Charles E. Merrill Books, Inc., 1964.

4. Fertis, D. G. and Zobel, E. C., Transverse Vibration Theory. The Ronald Press Company, 1961.

5. Goldsmith, W., Impact: The Theory and Physical Behaviour of Colliding Solids. Edward Arnold Publishers, Ltd., 1960.

6. Hoppmann, W. H., Impulsive Loads on Beams. Proceedings of the Society for Experimental Stress Analysis, v. 10, No. 1, November, 1951.

7. Murray, W. M. and Stein, P. K., Strain Gage Techniques. Massachusetts Institute of Technology Press, 1956.

8. Perry, C. C. and Lissner, H. R., The Strain Gage Primer. McGraw-Hill Book Company, Inc., 1962.

9. Schweiger, H. A., A Simple Calculation of the Transverse Impact on Beams and Its Experimental Verification. Proceedings of the Society for Experimental Stress Analysis, v. 22, No. 2, October, 1965.

INITIAL DISTRIBUTION LIST

		No. Copies
1.	Defense Documentation Center Cameron Station Alexandria, Virginia 22314	20
2.	Library, Code 0212 Naval Postgraduate School Monterey, California 93940	2
3.	Naval Ship Systems Command (Code 2052) Department of the Navy Washington, D. C. 20360	1
4.	Professor Eugene F. Lynch Department of Mechanical Engineering Naval Postgraduate School Monterey, California 93940	3
5.	Department of Mechanical Engineering Naval Postgraduate School Monterey, California 93940	2
6.	LTJG Thomas H. Berns, USN 1322 Monterey Ave., Norfolk, Va., 23508	1
7.	Mr. Ray Garcia Department of Mechanical Engineering Naval Postgraduate School Monterey, California 93940	1

Unclassified

Security Classification

DOCUMENT CONTROL DATA - R & D

(Security classification of title, body of abstract and indexing annotation must be entered when the overall report is classified)

1. ORIGINATING ACTIVITY (Corporate author)	2a. REPORT SECURITY CLASSIFICATION
Naval Postgraduate School Monterey, California 93940	Unclassified
	2b. GROUP

3. REPORT TITLE

Experimental Techniques for Analysis of Transverse Impact on Beams

4. DESCRIPTIVE NOTES (Type of report and inclusive dates)

Master's Thesis; June 1969

5. AUTHOR(S) (First name, middle initial, last name)

Thomas Herbert Berns

6. REPORT DATE	7a. TOTAL NO. OF PAGES	7b. NO. OF REFS
June 1969	64	9

8a. CONTRACT OR GRANT NO.	9a. ORIGINATOR'S REPORT NUMBER(S)
b. PROJECT NO.	
c.	9b. OTHER REPORT NO(S) (Any other numbers that may be assigned this report)
d.	

10. DISTRIBUTION STATEMENT

Distribution of this document is unlimited

11. SUPPLEMENTARY NOTES	12. SPONSORING MILITARY ACTIVITY
	Naval Postgraduate School Monterey, California 93940

13. ABSTRACT

Procedures are developed to facilitate laboratory investigation of the effects of short-duration transverse impact loading on simply supported beams. The particular beam investigated was aluminum, with constant rectangular cross-section. Six loading conditions were examined, consisting of a central impact from three heights for each of two spherical masses. Theoretical analysis was made of the frequency and deflection characteristics for ten equally spaced locations on the beam, under the assumption of Euler's beam theory. Experimental data were compared with theoretical values to give an indication of the effectiveness of the theoretical system in representing the physical system. It was concluded that the theory gives a good representation of the physical system, especially with respect to the frequency characteristics.

The experimental work was performed from January, 1969, through May, 1969, at the Naval Postgraduate School, Monterey, California.

DD FORM 1 NOV 65 1473 (PAGE 1)

S/N 0101-807-6811

Unclassified

Security Classification

A-31408

14 KEY WORDS	LINK A		LINK B		LINK C	
	ROLE	WT	ROLE	WT	ROLE	WT
Impact						
Free Vibration of Beams						